

Levels and Sources of Hydrocarbons in the Patos Lagoon Estuary and Cassino Beach Mud Bank (South Atlantic, Brazil): Evidence of Transference Between Environments

Patricia Andrade Neves

Universidade de São Paulo

Patricia G. Costa

Universidade Federal do Rio Grande

Luana C. Portz

Autonomous University of Madrid

Marina R. D. Garcia (✉ marinareback@gmail.com)

Universidade Federal do Paraná

Gilberto Fillmann

Universidade Federal do Rio Grande

Research Article

Keywords: hydrocarbons, PAHs, sediment cores, Patos Lagoon Estuary, mudbank

Posted Date: August 1st, 2022

DOI: <https://doi.org/10.21203/rs.3.rs-1871426/v1>

License:  This work is licensed under a Creative Commons Attribution 4.0 International License. [Read Full License](#)

Additional Declarations: No competing interests reported.

Version of Record: A version of this preprint was published at Environmental Monitoring and Assessment on March 18th, 2023. See the published version at <https://doi.org/10.1007/s10661-023-11074-3>.

Abstract

This study aimed to evaluate the concentrations and sources of natural and anthropogenic aliphatic (AHs) and polycyclic aromatic hydrocarbons (PAHs) in surficial sediments collected along the Patos Lagoon estuary and in sediment cores obtained from the Cassino Beach mud bank. Levels and distribution of *n*-alkanes indicate terrestrial sources, overlapping with a low amount of petrogenic hydrocarbons (heavy oils). A small unresolved complex mixture (UCM) was observed in all samples. On the other hand, the distribution of PAHs in the sediments showed a predominance of pyrolytic over petrogenic sources. In general, hydrocarbons (HCs) contamination in the Patos Lagoon estuary and its adjacent coastal area can be considered low, except for sites near urban or industrial effluents, where moderate to high levels of contamination were found. Concentrations of HCs were homogeneous throughout the sediment cores, suggesting that mixing processes may have occurred along the layers or that HCs inputs to the mud banks were uniform during the studied deposition period. In addition, the levels and profile of HCs levels in the coastal sediments were similar to those observed in the estuary, suggesting that HCs are promptly exported without any significant dilution and/or degradation during this process. Moreover, the frequent remobilization of sediments from the mud bank towards Cassino beach does not seem to pose any threats to the local biota or beach users since the levels of contamination were relatively low.

1 Introduction

Coastal zones are the receptors of many substances from natural processes and human activities (Kennish, 1997), ranging from organic matter to complex mixtures of synthetic organic and inorganic contaminants. As population density and economic activity in coastal regions increase, these environments are vulnerable to anthropogenic inputs that may lead to concerning levels of environmental contamination (Bay et al., 2003; Bayona and Albaigés, 2006; Bixian et al., 2001; Boonyatumanond et al., 2006; Hostettler et al., 1999). Among the most relevant and ubiquitous contaminant group, hydrocarbons (HCs) are chemical markers of land-based organic inputs (Volkman et al., 1992). Due to their partition coefficients, HCs preferentially accumulate in the particulate phases (Wu et al., 2001), making sediments the most suitable matrix for spatial and temporal studies.

In aquatic environments, HCs are commonly found as complex mixtures derived from numerous overlapping sources and are potentially deleterious to the environment (Goswani *et al.*, 2016; Ramzi *et al.*, 2016). The relative concentrations of aliphatic (AHs) and polycyclic aromatic (PAHs) hydrocarbons in sediments have been used to distinguish among different hydrocarbon sources (petrogenic, pyrogenic, biogenic and diagenetic). AHs are a major component of petroleum and its derivatives, although they can also be synthesized by algae and higher plants (Volkman et al., 1992; Meyers, 1997; Kumar et al., 2016). PAHs are mostly derived from anthropogenic sources, specifically the incomplete combustion of organic matter (fossil fuel, coal, wood) and the spillage of petroleum and its byproducts (Readman et al., 2002; Ravindra et al., 2008, Chen and Chen, 2011, Zhang et al., 2015).

Estuaries are important transition zones between fluvial and marine systems that can act as temporary or permanent traps for anthropogenic contaminants. The sediment balance between inputs of terrestrial or adjacent coastal zones and outputs relies on the local hydrodynamics of tides, waves and river flows (Langston and Ridgway, 2006). Since many contaminants may adversely affect estuarine and coastal ecosystems, it is important to increase knowledge of their distribution, concentration, transference processes and impacts (Ridgway and Shimmield, 2002).

The Patos Lagoon (PL), located on the southern Brazilian coast (30–32 °S), is the world's largest choked coastal lagoon (Kjerfve, 1986) (Fig. 1). The estuarine region, which covers approximately 10% of the total area, has great economic and ecological importance due to its high productivity (Seeliger, 2001). This area, however, has been subject to intense anthropogenic pressure related to maritime (Rio Grande port complex is the second largest in Brazil), industrial (oil refinery, fertilizers plants, food industries, etc.) and urban activities (the cities of Rio Grande and São José do Norte used to discard untreated sewage into the estuarine waters) (Wallner-Kersanach et al., 2016). Its riverine tributaries, running off organic matter from extensive natural grasslands (Boldrini and Eggers, 1996), provide a large amount of fine sediments to the PL system. According to the hydrodynamics, these fine materials can be trapped in the estuary or carried out to the adjacent coastal areas (Dyer, 1988; Burchard et al., 2018). As a result, a large mud deposit (mudbank) has formed south of Patos Lagoon output (offshore Cassino Beach), mostly between the 6 and 20 m isobaths (Calliari et al., 2009). During severe storm events, mudbank sediments can be remobilized and transported to the shoreface and/or beach (Calliari *et al.*, 2000), which could potentially be linked to dredging operations in Rio Grande port; however, this is still a controversial topic (Mirlean et al., 2020; Garcia et al., 2021). As fine sediments are able to adsorb and accumulate contaminants, local biota and beach users at Cassino Beach might be under threat.

Previous studies have shown moderate to high concentrations of hydrocarbons in estuarine sediments near the main sources of contamination (domestic/industrial sewages and harbor activities) (Medeiros et al., 2005; Garcia et al., 2010). However, neither the processes of transference of hydrocarbons from the estuarine system to the adjacent coast nor their levels in the adjacent coastal depositional areas have been previously appraised. Thus, the present study assessed the levels and sources of hydrocarbons to address evidence of processes of transport, dilution and degradation of these compounds from the estuary to the adjacent coastal mudbank. Levels and sources of HCs were discussed in the face of the estuarine morphology and depositional aspects of the mudbank.

2 Methodology

2.1 - Sampling

Superficial sediment samples (top 2 cm) were collected inside the Patos Lagoon estuary using a stainless-steel grab and stored in pre-cleaned aluminum jars (-15°C) until analysis. Sediment samples 1 to 17 were collected in 2003, while samples 18 to 27 were collected in 2006 and 2007 (Fig. 1). In addition, four sediment cores were collected in 2005 by scuba diving in the mud bank located in front of Cassino beach (Fig. 1) (Vinson et al., 2009). The locations and descriptions of the sampling sites are available in Table S1 of the Supporting Information. In the laboratory, cores were sliced into 2 cm layers to obtain

interposed samples for grain size analysis, total organic carbon, age-dating and hydrocarbon determinations. Samples were placed in precleaned aluminum jars and stored at -15°C until analyses.

2.2 - Analysis

2.2.1 - Bulk parameters

Sedimentation rates and sediment radiochronology were determined based on the relative concentrations of ^{210}Pb and/or ^{137}Cs , as described by Gale et al. (1995) and Reed et al. (2009). Total organic carbon (TOC) was determined using a CHNS Perkin-Elmer 2400 Serie II, according to Yang et al. (1998). Grain size and sediment density analyses were performed as described by Gray (1981).

2.2.2 - Analysis of Hydrocarbons

All samples were freeze-dried and analysed within 1 year of sampling, as described by Niencheski and Fillmann (2006). Briefly, 15 g of dried sediments was spiked with surrogate standards (1-hexadecene and 1-eicosene and *p*-Terphenyl- D_{14}) and Soxhlet-extracted for 12 h with *n*-hexane/dichloromethane (1:1) after stabilization. Extracts were concentrated (~ 1 mL), and activated copper was added to remove sulfur. Extracts were then cleaned up and fractionated using a column of silica gel (6 g) and neutral aluminum oxide (8 g, deactivated with 5% water). Elution was performed using 25 mL of hexane to yield the first fraction (which contains the AHs – F1), followed by 30 mL of *n*-hexane/dichloromethane (90:10) and 25 mL of *n*-hexane/dichloromethane (50:50) (which combined contain the PAHs – F2). Fractions F1 and F2 were concentrated, transferred to vials and fortified with internal standards for AHs or PAHs. The final volume was adjusted to exactly 1 mL using N_2 , and an aliquot of 1 μL of each extract was analyzed by GC-FID (F1) and GC-MS (F2).

AHs (F1) were analyzed on a Perkin Elmer Clarus 500 gas chromatograph equipped with a flame ionization detector (GC-FID), an autoinjector and a capillary column Elite-1 (100% dimethylpolysiloxane; 30 m x 0.25 mm x 0.25 μm film thickness). Helium was used as the carrier gas (1.5 mL min^{-1}). The injector temperature was maintained at 280°C in splitless mode, while the GC temperature was programmed from 40°C to 290°C at 5°C min^{-1} , maintained at 290°C for 10 min, increased to 300°C at 10°C min^{-1} , and then held at 300°C for 10 minutes.

PAHs analyses were carried out using a gas chromatograph coupled with a mass spectrometer (Perkin Elmer Clarus 500 – GC-MS) using an Elite-5MS silica capillary column (5% phenyl-95% methylpolysiloxane; 30 m x 0.25 mm, 0.25 μm film thickness). The injector was kept at 280°C in splitless mode. The GC temperature was programmed from 40°C to 60°C at 10°C min^{-1} , from 60°C to 290°C at 5°C min^{-1} , maintained at 290°C for 5 min, increased to 300°C at 10°C min^{-1} , and then held at 300°C for 10 min. Helium was used as the carrier gas (1.5 mL min^{-1}). Ion source and transfer line temperatures were set at 290°C, and 70 eV was used for ionization. Selected ion monitoring mode was used for quantification. Data acquisition was performed in SIFI (Selected Ion and Full Ion Scanning).

Compound identification was based on individual mass spectra and GC retention times in comparison to library data and authentic standards (Supelco). Instrumental calibration was performed for 23 PAHs with solutions containing naphthalene (Nap), 2-methylnaphthalene (2-MN), 1-methylnaphthalene (1-MN), 1,7-dimethylnaphthalene (1,7-DMN) and 2,6-dimethylnaphthalene (2,6-DMN), acenaphthylene (Acy), acenaphthene (Ace), fluorene (Fl), phenanthrene (Phe), methylphenanthrene (C1Phe), anthracene (Ant), fluoranthene (Flu), pyrene (Pyr), benz[a]anthracene (BaA), chrysene (Chr), benzo[b]fluoranthene (BbF), benzo[k]fluoranthene (BkF), benzo[a]pyrene (BaP), indeno[1,2,3-cd]pyrene (InP), dibenz[a,h]anthracene (DBA), benzo[ghi]perylene (BP), benzo[e]pyrene (BeP), and perylene (Per) at different concentrations (5, 10, 20, 50, 100, 250 and 500 ng mL^{-1}). For AHs, the calibration was made with $n\text{C}_{10-36}$, pristane and phytane at 0.5, 1, 2, 4, 8, 12, 15, 20, 25 and 50 $\mu\text{g mL}^{-1}$. Compound quantitation was performed using the following internal standards: 1-tetradecene (for AHs), naphthalene-D8, acenaphthene-D10, phenanthrene-D10, chrysene-d12 and perylene-D12.

Quantification of PAHs in samples included 23 individual compounds: parental PAHs naphthalene (Nap), acenaphthylene (Acy), acenaphthene (Ace), fluorene (Fl), phenanthrene (Phe), anthracene (Ant), fluoranthene (Flu), pyrene (Pyr), benz[a]anthracene (BaA), chrysene (Chr), benzo[b]fluoranthene (BbF), benzo[k]fluoranthene (BkF), benzo[a]pyrene (BaP), indeno[1,2,3-cd]pyrene (InP), dibenz[a,h]anthracene (DBA), benzo[ghi]perylene (BP), benzo[e]pyrene (BeP), and perylene (Per); and alkylated PAHs 2-methylnaphthalene (2-MN), 1-methylnaphthalene (1-MN), 2-methylnaphthalene (2-MN), 1-methylnaphthalene (1-MN) and methylphenanthrene (C1Phe).

Quality assurance and quality control were based on regular analyses of blanks, spiked matrices and certified reference material (IAEA-417). Recoveries for surrogate standards varied between 40 and 100%, while for CRM-IAEA-417, they were between 70 and 112% (n = 10). Limits of quantitation (LOQ) were the lowest quantifiable concentration of the calibration curve (0.3 ng g^{-1} for PAHs and 0.03 $\mu\text{g g}^{-1}$ for AHs).

3 Results And Discussion

AHs and PAHs results for Patos Lagoon estuary and Cassino Beach mudbank samples are shown in Table 1 and Figs. 2 and 3. Some of the sediments were sampled near potential hydrocarbon sources, while other samples were collected in areas located away from these sources. AHs concentrations were not determined for sites 18 to 27, since these sites were originally used exclusively to assess the PAHs levels associated with activities at Rio Grande port.

3.1 - PATOS LAGOON ESTUARY

3.1.1 - Aliphatic Hydrocarbons

Concentrations of total aliphatic hydrocarbons (total AHs) – comprehending the resolved aliphatic fraction plus the unresolved complex mixture (UCM) – varied from 0.68 to 3,383 $\mu\text{g g}^{-1}$ dry weight (d.w.) (Fig. 2). According to Volkman et al. (1992), total AHs concentrations above 100 $\mu\text{g g}^{-1}$ are generally associated with oil inputs to the environment, and values above 500 $\mu\text{g g}^{-1}$ are indicative of chronic hydrocarbon contamination. According to these thresholds, sites 2 (marina), 3 (city market) and 4 (dry docking) probably contain a degree of oil inputs, while sites 6 (Sewage), 7 (petroleum distributor) and 8 (petroleum refinery) can be considered chronically contaminated by hydrocarbons.

The total AHs concentrations were below 10 $\mu\text{g g}^{-1}$ at sites 1 (Pombas Island), 11, 12, 13 (Marinheiros Island), 14, 16 and 17 (Mangueira Cove). Such values (and even higher in areas with significant biogenic inputs) are similar to concentrations reported for areas considered to be free of contamination (Volkman et al., 1992; Readman et al., 2002; Dauner et al., 2015). No correlation was observed between total AHs concentrations and grain size ($r_s = -0.55$; $p > 0.05$) or between total AHs and TOC ($r_s = -0.53$; $p > 0.05$).

UCM concentrations varied between < LOQ (limit of quantification) and 3,353 $\mu\text{g g}^{-1}$ (d.w.). The presence of UCM is generally associated with degraded or weathered oil residues (Readman et al., 2002; White et al., 2013), being formed by resistant molecules that tend to accumulate in the sediment (Bouloubassi and Saliot, 1991). UCM was present in 62% of the stations, representing 76 to 99% of the total AHs (Table 1). High levels of total AHs and predominance of UCM suggest chronic oil input at sites 2 (marina), 3 (city market), 4 (dry docking), 6 (sewage), 7 (petroleum distributor) and 8 (petroleum refinery). Additional evidence of chronic oil introduction is provided by the ratio between UCM and resolved aliphatics, with results above 4 indicating contributions of degraded oil products (Yunker et al., 2002). Most sites showed results above 4, and very high ratios were observed at sites 3 (55.96), 6 (124.31) and 7 (109.97) (Table 1), while at 5 stations, the ratio was 0 (10, 11, 12, 13, 15 and 16) (Table 1). Although UCM has also predominated at sites 5 (Fertilizer industry), 9 (Mangueira Cove 1), 10 (Oil Terminal), 14 (Mangueira Cove 2) and 15 (Mangueira Cove 3), the total AHs levels were low and similar to those found in nonpolluted areas (Wang et al., 1999; Medeiros and Bicego, 2004; Massone et al., 2013).

The sum of $n\text{-C}_{12-36}$ alkanes ranged between 0.28 and 36.4 $\mu\text{g g}^{-1}$ (d.w.) (Table 1). The concentrations of the n -alkanes observed in the estuarine sediments of Patos Lagoon were higher than those observed in previous studies (0.2–7.5 $\mu\text{g g}^{-1}$; Medeiros et al., 2005). The results obtained are on the same order of magnitude as those reported for other locations in Brazil under moderate human impact (6.04–44.0 $\mu\text{g g}^{-1}$; Martins et al., 2015; 4.2–55.6 $\mu\text{g g}^{-1}$; Assunção et al., 2017) but lower than places considered heavily impacted, such as Guanabara Bay, Brazil (3.0–318 $\mu\text{g g}^{-1}$; Farias et al., 2008) and Malacca Strait, Malaysia (28.0–254.5 $\mu\text{g g}^{-1}$; Vaezzadeh et al., 2015). However, pristine locations can also present similar or higher levels of n -alkanes when compared to the Lagoa dos Patos estuary, such as Camamu, Brazil (0.77–55.17 $\mu\text{g g}^{-1}$; Paixao et al., 2011) and Kerala, India (10.3–221.4 $\mu\text{g g}^{-1}$; Resmi et al., 2016).

Individual n -alkane distributions revealed the predominance of odd long chain n -alkanes ($n\text{-C}_{29}$ and $n\text{-C}_{31}$) at most stations, suggesting a biogenic contribution from terrigenous sources (higher plant waxes) (Eglinton and Hamilton, 1967; Volkman et al., 1992; Medeiros and Bicego, 2004). This is confirmed by the predominance of n -alkanes associated with terrestrial sources (alk_{terr}) at most sites (Table 1): $n\text{-C}_{31}$ showed the highest concentrations at most sites, indicating inputs from C4-type grasses (Schefuß et al., 2003; Bush and McInerney, 2015) from both salt marshes of the Patos Lagoon estuary (e.g., *Spartina alterniflora*, *Spartina densiflora*, etc.) (Marangoni and Costa, 2009) and the runoff of the extensive natural grasslands along the Patos Lagoon drainage area (Boldrini and Eggers, 1996).

Table 1
 Concentrations of total aliphatic hydrocarbons (AHs), sum of alkanes, UCM, total PAHs, perylene, total organic carbon, fine sediments and selected diagenetic products sampled in the Patos Lagoon Estuary and Cassino beach mudbank.

Station	Total AHs	$\sum nC_{12-36}$	UCM	UCM/RA	TAR	ACL	P_{aq}	CPI	alk _{terr}	$\Sigma_{23}HPAs$	%PER/ 5-ringPAH	2-3 rings/ 4-6 rings	FLU/ FLU + PYR	ANT/ ANT + PHE	ID/ ID + BPER
	($\mu g g^{-1}$)	($\mu g g^{-1}$)	($\mu g g^{-1}$)						(%)	($ng g^{-1}$)					
1	0.75	0.46	<LOQ	9.05	0.19	28.39	0.20	1.61	n.c.	38.25	21.15	3.65	0.54	n.c.	0.6
2	206.62	5.95	186.06	5.05	2.65	28.46	0.15	4.49	49.43	872.25	15.96	0.55	0.55	0.9	n.c.
3	261.52	17.86	218.3	55.96	0.63	27.78	0.28	2.13	20.94	336.77	51.56	1.24	0.47	0.49	0.5
4	354.95	4.01	329.07	9.67	2.08	28.25	0.21	2.84	38.19	2327.88	11.68	0.61	0.56	0.68	0.58
5	52.58	1.84	47.65	7.04	4.10	28.32	0.21	3.71	55.73	844.56	16.02	3.92	0.59	0.99	n.c.
6	573.13	36.42	501.88	124.31	2.91	28.11	0.21	1.83	38.88	394.07	42.03	0.52	0.48	0.3	0.53
7	1388.43	2.29	1377.35	109.9	2.10	28.39	0.19	2.59	43.20	329.33	6.50	0.09	0.28	n.c.	0.01
8	3383.55	7.12	3353.06	3.28	1.56	28.58	0.18	2.72	36.38	580.46	27.98	0.34	0.44	0.59	0.44
9	16.49	1.61	12.64	7.43	4.30	28.42	0.20	3.30	53.90	45.89	59.97	0.55	0.51	n.c.	0.48
10	23.95	0.75	21.11	n.c.	4.09	28.01	0.25	2.86	52.21	154.43	22.76	0.41	0.54	n.c.	0.5
11	1.11	0.53	<LOQ	n.c.	0.51	28.35	0.18	1.37	23.55	1.96	56.72	0.76	0.58	n.c.	0.6
12	0.91	0.44	<LOQ	n.c.	0.33	28.89	0.14	1.42	13.93	25.74	65.71	198.75	n.c.	n.c.	n.c.
13	0.68	0.38	<LOQ	8,06	0.54	27.94	0.28	1.58	16.24	4.02	52.63	0.91	0.6	n.c.	0.6
14	14.4	0.63	12.81	6,95	7.23	28.03	0.23	2.09	69.13	9.28	77.88	10.56	0.47	n.c.	0.5
15	15.83	0.88	13.84	n.c.	2.53	28.32	0.19	5.95	64.77	5.39	54.42	0.43	0.51	n.c.	0.4
16	1.65	0.45	<LOQ	n.c.	0.56	28.05	0.24	3.33	30.33	9.76	4.67	0.10	0.43	n.c.	0.31
17	0.70	0.28	<LOQ	16,91	2.97	29.65	0.11	2.42	67.80	14.45	n.c.	154.89	n.c.	n.c.	n.c.
18	Data not available									122.24	83.39	0.56	0.6	4.91	n.c.
19	Data not available									56.66	72.01	0.91	0.56	3.72	n.c.
20	Data not available									148.82	77.62	0.49	0.57	6.43	n.c.
21	Data not available									165.07	70.58	0.50	0.56	5.8	n.c.
22	Data not available									96.15	81.51	0.61	0.57	4.74	n.c.
23	Data not available									89.75	73.65	0.58	0.57	n.c.	n.c.
24	Data not available									142.16	80.28	0.45	0.58	5.27	n.c.
25	Data not available									182.38	65.89	0.49	0.58	13.65	n.c.
26	Data not available									59.14	88.59	1.88	0.57	n.c.	n.c.
27	Data not available									81.66	76.37	2.56	0.54	4.44	n.c.

<LOQ: below the quantitation limit; n.c. : not calculated; $\sum nC_{12-36}$: sum of n-alkanes n-C₁₂ to n-C₃₆; UCM: Unresolved Complex Mixture; UCM/RA: UCM/Reso (n-C₂₉ + n-C₃₁)/(n-C₁₅ + n-C₁₇ + n-C₁₉); ACL: ((23*n-C₂₃)+(25*n-C₂₅)+(27*n-C₂₇)+(29*n-C₂₉)+(31*n-C₃₁))/(n-C₂₃ + n-C₂₅ + n-C₂₇ + n-C₂₉ + n-C₃₁); P_{aq} : (n-C₂₃ + n-C₂₉ + n-C₃₁); CPI: (0,5*(\sum odd n-C₂₅ - n-C₃₃/ \sum even n-C₂₄ - n-C₃₂)+(\sum odd n-C₂₅ - n-C₃₃/ \sum even n-C₂₆ - n-C₃₄)); alk_{terr}: percentage of n-C₂₇, n-C₂₉, n-C₃₁ and n-C₃₆; $\Sigma PAHs_{23}$: sum of 23 PAHs; PER: Perylene; FLU: Fluoranthene; PYR: pyrene; ANT: anthracene; PHE: phenantrene; ID: Indeno(123)pyrene; BPER: Benzo(g benzo[a]anthracene; CHR: chrysene; TOC: total organic carbon.

Table 1

(Cont.): Concentrations of total aliphatic hydrocarbons (AHs), sum of alkanes, UCM, total PAHs, perylene, total organic carbon, fine sediments and selected dia sampled in the Patos Lagoon Estuary and Cassino beach mudbank.

	Depth (cm)	Total AHs ($\mu\text{g g}^{-1}$)	$\sum n\text{C}_{12-36}$ ($\mu\text{g g}^{-1}$)	UCM ($\mu\text{g g}^{-1}$)	UCM/RA	TAR	ACL	P_{aq}	CPI	Alkterr (%)	$\Sigma_{23}\text{HPAs}$ (ng g^{-1})	%PER/5-ringPAH	2-3 rings/4-6 rings	FLU/FLU + PYR	ANT/ANT + PHE	ID/ID + BPER
Core 1	2,5-5	20.31	0.81	15.40	3.14	n.c.	29.00	0.12	3.73	66.70	15.17	80.13	0.35	0.53	n.c.	0.53
	17,5-21	29.30	1.34	23.08	3.71	n.c.	28.42	0.21	2.68	56.41	15.05	72.89	0.27	0.51	n.c.	0.52
	34,5-37,5	25.47	1.08	19.52	3.28	n.c.	28.32	0.22	2.22	52.86	7.58	72.36	0.37	0.51	n.c.	n.c.
	43,5-45	22.26	0.93	16.24	2.70	n.c.	27.91	0.28	1.91	47.46	14.42	79.87	0.28	0.51	n.c.	0.53
	60-62	32.18	1.30	23.59	2.74	n.c.	28.70	0.18	3.28	61.40	33.35	80.51	0.28	0.52	n.c.	0.50
Core 2	0-3	21.40	0.07	11.53	0.87	n.c.	30.01	n.c.	n.c.	100.00	0.85	100.00	n.c.	n.c.	n.c.	n.c.
	10-13	11.62	<LOQ	9.40	4.24	n.c.	n.c.	n.c.	n.c.	n.c.	<LOQ	n.c.	n.c.	n.c.	n.c.	n.c.
	20-23	29.51	1.49	22.25	3.06	n.c.	28.84	0.14	3.57	64.65	17.42	77.60	0.33	0.56	n.c.	n.c.
	30-33	18.57	0.95	12.88	2.27	n.c.	28.89	0.14	2.20	56.91	8.29	83.35	0.68	0.57	n.c.	n.c.
	40-43	21.40	1.72	13.19	1.61	n.c.	28.12	0.23	1.70	48.29	18.48	81.80	0.48	0.54	n.c.	n.c.
	50-53	31.23	0.79	12.95	0.71	n.c.	28.21	0.20	1.41	46.76	6.27	82.49	0.38	0.55	n.c.	n.c.
	60-63	18.39	0.96	13.06	2.45	n.c.	28.27	0.23	2.22	52.95	10.72	88.22	0.33	0.58	n.c.	n.c.
Core 3	0-2	35.96	1.72	28.83	4.05	n.c.	28.59	0.18	3.11	58.10	119.53	87.85	0.55	0.53	0,28	0.49
	6-8	26.27	1.20	21.26	4.24	n.c.	28.51	0.19	3.19	60.86	69.23	75.69	0.59	0.51	0,34	0.53
	16-18	27.31	1.67	20.60	3.07	n.c.	28.40	0.20	2.99	57.82	97.95	81.44	0.47	0.55	0.27	0.59
	23-30	31.48	1.93	24.22	3.34	n.c.	28.52	0.19	3.40	59.90	97.62	75.62	0.42	0.55	0.26	0.53
	33-40	31.23	2.77	27.64	2.47	n.c.	28.38	0.20	2.48	54.07	106.15	77.57	0.41	0.57	0.28	0.54
	43-50	34.20	1.40	19.58	3.17	n.c.	28.60	0.17	3.15	61.50	69.52	76.40	0.46	0.54	0.28	0.52
	53-60	31.65	1.96	25.97	3.15	n.c.	28.56	0.17	2.89	59.39	93.91	72.25	0.36	0.52	0.25	0.52
Core 4	0-2	29.67	1.71	22.61	4.05	n.c.	28.72	0.17	3.52	62.04	14.49	80.55	0.29	0.54	n.c.	0.57
	6-10	26.31	1.91	18.87	4.24	n.c.	28.48	0.18	2.23	54.73	12.64	75.32	0.38	0.55	n.c.	0.50
	13-20	22.78	0.67	18.86	3.07	n.c.	28.85	0.13	2.86	62.09	7.11	78.41	0.58	0.55	n.c.	n.c.
	23-30	30.57	1.74	22.93	3.34	n.c.	28.43	0.20	2.37	54.72	12.62	70.80	0.33	0.53	n.c.	0.58
	33-40	29.45	0.76	25.19	2.47	n.c.	29.04	0.11	3.52	66.95	8.72	69.46	0.44	0.53	n.c.	n.c.
	45-50	32.49	1.24	26.78	3.17	n.c.	28.77	0.15	3.55	64.32	11.79	72.48	0.28	0.49	n.c.	0.52
	53-60	31.76	1.64	24.05	3.15	n.c.	28.27	0.21	1.85	50.42	17.47	67.51	0.26	0.50	n.c.	0.53

<LOQ: below the quantitation limit; n.c. : not calculated; $\sum n\text{-C}_{12-36}$: sum of n-alkanes n-C₁₂ to n-C₃₆; UCM: Unresolved Complex Mixture; UCM/RA: UCM/Reso C₂₉ + n-C₃₁ / (n-C₁₅ + n-C₁₇ + n-C₁₉); ACL: ((23*n-C₂₃) + (25*n-C₂₅) + (27*n-C₂₇) + (29*n-C₂₉) + (31*n-C₃₁)) / (n-C₂₃ + n-C₂₅ + n-C₂₇ + n-C₂₉ + n-C₃₁); P_{aq} : (n-C₂₃ + n-C₂₅ + n-C₃₁); CPI(nC₂₅₋₃₅): (0,5*((\sum odd n-C₂₅ - n-C₃₃) / \sum even n-C₂₄ - n-C₃₂) + (\sum odd n-C₂₅ - n-C₃₃) / \sum even n-C₂₆ - n-C₃₄)); alkterr: percentage of n-C₂₇, n-C₂₉, n-C₃ C₁₂ - n-C₃₆; Σ PAHs₂₃: sum of 23 PAHs; PER: perylene; FLU: Fluoranthene; PYR: pyrene; ANT: anthracene; PHE: phenantrene; ID: Indeno(123)pyrene; BPER: B benzo[a]anthracene; CHR: chrysene; TOC: total organic carbon.

The CPI (carbon preference index, nC_{24}/nC_{35}) was calculated to further verify the predominant source of *n*-alkanes. According to Bi et al. (2005), CPI values above 2.3 suggest the predominance of higher plants, while CPI values close to 1 usually imply the predominance of anthropogenic *n*-alkanes derived from oil contamination (Aboul-Kassim and Simoneit, 1996). However, some studies suggest that a CPI below 1.5 can also indicate planktonic inputs as the main source of *n*-alkanes (Fahl and Stein, 1997; Clark and Blumer, 1967). In the present study, most sediments presented CPI ratios above 2.3, suggesting the predominance of higher plants (Table 1). CPI ratios, however, were close to 1 at sites 1 (Pombas Island), 11, 12 and 13 (Marinheiros Island). These sites also presented low levels of total AHs and no UCM, suggesting that *n*-alkanes from planktonic sources were more likely than petrogenic inputs. nC_{17} was also observed at most sites, suggesting that planktonic inputs from algal blooms (Chevalier et al., 2015; Yunes et al., 1996) were another probable source of *n*-alkanes inside the lagoon.

The terrigenous/aquatic ratio (TAR) evaluates the terrigenous inputs versus aquatic inputs $[(nC_{27} + nC_{29} + nC_{31})/(nC_{15} + nC_{17} + nC_{19})]$, where values above 1.0 correspond to terrigenous material (Bourbonniere and Meyers, 1996; Silliman et al., 1996; Vaezzadeh et al., 2015). Although the ratios varied between 0.19 and 7.23, most sites showed values indicating terrigenous sources, as seen for CPI ratios. Ratios for sites 1 (Pombas Island), 11, 12 and 13 (Marinheiros Island), as also seen for CPI ratios, indicated aquatic inputs. The ratios for sites 3 and 16 also indicated aquatic sources.

The proxy P_{aq} (aquatic macrophytes/emergent and terrestrial species) uses the relative proportion of mid chain to long chain homologues (Ficken et al., 2000; Ankit et al., 2017). $P_{aq} < 0.1$ corresponds to terrestrial plants, 0.1–0.4 to mixed sources and > 0.4 –1 to submerged/floating macrophytes. P_{aq} ratios varied between 0.11 and 0.28, remaining on the mixed sources range and, therefore, showing little differentiation along the sampling area.

The average chain length (ACL) reflects the average number of carbon atoms for *n*-alkanes (Jeng, 2006; Bush, 2013; Vaezzadeh et al., 2015), where nC_{23} and nC_{25} are found in sediments to Sphagnum mosses, nC_{27} and nC_{29} to woody plants, and nC_{31} to graminoids (grasses), although the signals of the last two groups may be mixed in the sediments. In the present study, the ACL ranged from 27.8 to 29.6, indicating a mixed source of both woody plants and graminoids.

3.1.2 - Polycyclic Aromatic Hydrocarbons

Total PAHs (Σ_{23} PAH) concentrations ranged from 1.96 to 2,303 $ng\ g^{-1}$ (d.w.) (Fig. 3) in the Patos Lagoon estuary. These results were slightly lower than those previously observed by Medeiros et al. (2005) for the same study area (Σ_{23} PAH – 37.7 to 11,780 $ng\ g^{-1}$ (d.w.)), similar to those reported for other locations in Brazil under moderate human impact (15.1–1,013 $ng\ g^{-1}$, Martins et al., 2015; $ng\ g^{-1}$; 26.0–434; Assunção et al., 2017), and lower than levels found in heavily contaminated estuaries, such as Guanabara Bay (10–240,394 $ng\ g^{-1}$; Farias et al., 2008) and Fortaleza (3,040–2,234,760 $ng\ g^{-1}$; Cavalcante et al., 2009).

Based on Σ PAH levels, sites can be divided into 3 groups: i) Highly contaminated - sites 2 (marina), 4 (dry docking), 5 (fertilizer industry), and 8 (petroleum refinery) showed concentrations above 500 $ng\ g^{-1}$, characteristic of chronically contaminated environments (Notar et al., 2001); ii) Moderately contaminated - sites 3 (city market), 6 (sewage), 7 (petroleum distributor), 10 (oil terminal), 18 (São José do Norte), 20 (Rio Grande new port) to 25 (pilot house) and 27 (jetty outer edge); iii) Low contaminated - sites 1 (Pombas island), 9 (Mangueira cove 1), 11 (Marinheiros island 1) to 17 (Mangueira cove 5), 19 (old port) and 26 (inner jetty edge) (Fig. 3). As seen for total AHs, no correlation was found between PAHs concentration vs grain size ($r_s = 0.42$; $p > 0.05$) and PAHs concentration vs TOC ($r_s = 0.34$; $p > 0.05$).

Petrogenic inputs usually have a high proportion of lower molecular weight PAHs (LMW – 2 to 3 aromatic rings) and a great abundance of alkylated homologues, while high molecular weight PAHs (HMW – 4 to 6 rings) prevail in pyrogenic inputs (Neff, 1979). The ratio of HMW/LMW PAHs (Table 1) indicated that HMW PAHs predominated, except for sites 1 (Pombas Island), 3 (city market), 5 (fertilizer industry), 14 (Mangueira Cove 2) and 19 (old port), 26 (inner jetty edge) and 27 (outer jetty edge), where LMW PAHs concentrations were higher.

Molecular indexes (ratios between specific PAHs) can be used to assess the sources of PAHs introduced into the environment, taking into account their thermodynamic characteristics and the proportions of compounds found in the emissions sources and sediments (Yunker et al., 2002; Goswami et al., 2016; Ramzi et al., 2017). In the present study, four indexes were used according to Yunker et al. (2002). Benzo(a)Anthracene/Benzo(a)Anthracene + Chrysene ratio (BaA/(BaA + CHR)) helps to distinguish between inputs of oil (< 0.2), combustion (> 0.35), and the mixture between the former, while the anthracene/anthracene + phenanthrene ratio (ANT/(ANT + PHE)) differentiates between petrogenic (< 0.1), fossil fuel combustion (0.1–0.2) and combustion (> 0.2) inputs. For the fluoranthene/fluoranthene + pyrene ratio (FLU/(FLU + PYR)), values of > 0.5 indicate grass, wood and coal combustion, values between 0.5 and 0.4 indicate combustion of fossil fuels and values < 0.4 are indicative of oil inputs. The Indene[1,2,3-c,d]Pyrene/Indene[1,2,3-c,d]Pyrene + Benzo[ghi]Perylene ratio (ID/(ID + BPER)) differentiates between petrogenic (< 0.2), fossil fuel combustion (0.2 and 0.5) and grass, wood and coal combustion inputs (> 0.5). In the present study, PAHs ratios indicated the predominance of pyrogenic inputs, specifically wood, grass or coal combustion, to the lagoon (Fig. 4). However, the ANT/(ANT + FEN) and BaA/(BaA + CRI) ratios indicated petrogenic inputs for some sites, which indicates a mixture of pyrolytic and petrogenic sources to the estuary (Yunker et al., 2002; Martins et al., 2011).

Perylene is a major diagenetic PAH commonly found in marine sedimentary environments that can also be used as a marker (Silliman et al., 1998). Although its diagenetic precursors are associated with terrestrial organic matter (Vanosferany *et al.*, 2014), pyrogenic processes may yield perylene as well, and such an origin may be dominant in areas receiving high anthropogenic inputs. Its occurrence in levels $> 10\%$ of the total penta-aromatic PAHs isomers is attributed to diagenetic sources (Oyo-Ita et al., 2013; Baumard, 1998; Venkatesan, 1988). In the study area, perylene was observed at all sites, ranging from $< LOQ$ to 81.65 $ng\ g^{-1}$ (d.w.). Only 2 out of 27 sites (7 – petroleum distributor and 16 – Mangueira cove 4) showed proportions lower than 10% of the bulk PAHs, suggesting a predominance of pyrogenic sources for perylene at these specific sampling stations. In the majority of the sampling area, diagenetic sources were prevalent.

Sediment quality guidelines are broadly used to assess the contamination of aquatic environments. According to Buchman (2008), TEL (Threshold Effect Level) levels are values below which effects on organisms are rarely expected, while PEL (Probable Effect Level) indicates values above which effects on

organisms are frequently expected. All 27 sites showed concentrations of total PAHs below PEL ($\Sigma\text{PAH} < 16,770 \text{ ng g}^{-1}$), while one site (4 - dry docking) presented levels above TEL ($\Sigma\text{PAH} > 1,684 \text{ ng g}^{-1}$). In addition, according to the Brazilian guideline (Brasil, 2012), the sum of PAHs should not exceed 4,000 ng g^{-1} for saline/brackish sediment; therefore, none of the sites surpassed this level of contamination.

3.1.3 – Hydrocarbons distribution

Overall, the AHs and PAHs concentrations inside the Patos Lagoon estuary were higher at those sites under the influence of potential sources of hydrocarbons (e.g., sites 2–10). These sites are subject to oceanographic conditions (e.g., flocculation), which favor the deposition of hydrocarbons generated in the vicinity of their sources. No significant correlation was observed between the hydrocarbons found in the sites inside the lagoon and either grain size or TOC, which suggests that source proximity is probably the main cause of hydrocarbon concentration.

Medeiros et al. (2005) have previously assessed hydrocarbon concentrations and sources in 10 out of the 27 sites examined in the present study (sites 1–8, 10 and 26). Compared to the results obtained by Medeiros *et al.*, the concentrations of PAHs found in the present study were lower at sites 7 and 8 and slightly lower at the other sites, indicating that the study area can still be considered moderate to highly contaminated by hydrocarbons. The contamination levels at these 10 specific sites were similar to those found in other areas considered moderate to highly contaminated with hydrocarbons, such as the Pearl River estuary in China (Zhang et al., 2015), the Iko River estuary mangrove system in Nigeria (Essien et al., 2011) and the Cochin estuary in India (Ramzi *et al.*, 2016).

Intermediate levels of PAHs were observed in sites located along the main navigation channel, directly influenced by maritime activities (sites 18–27). These sites, despite being close to expected sources of PAHs, are subjected to stronger currents (Martelo et al., 2019, Antonio *et al.*, 2020), which apparently can dilute the contamination and/or prevent sediment and hydrocarbon deposition (Janeiro et al., 2008), resulting in the intermediate concentrations observed. Lower AHs and PAHs concentrations were observed in sites located in areas far from the expected sources (sites 1, 11–13) or with low contents of fine sediments, such as Manguieira Cove (sites 14–17). Hydrocarbon concentrations at these specific sites were comparable to those found in areas considered unpolluted, such as Admiralty Bay in Antarctica (Martins et al., 2010) and Laranjeiras Bay (marine protected area) in Brazil (Martins et al., 2012).

3.2 - SEDIMENT CORES OF CASSINO BEACH MUBANK

The fine sediments originating inside the lagoon are transported southward by coastal drift and settle offshore, forming the Cassino beach mudbank (Calliari et al., 2007). The mudbank sediments are periodically remobilized and transported to the beach during high-energy events (storms) caused by cold fronts (Calliari et al., 2009). In these situations, the beach can be covered in mud, affecting local tourism and the biota.

Currents and waves modify the mud deposit by transporting and suspending the sediments, influencing the mud density and sorting the mud by grain size. As wave and current shear forces progressively decrease, the mud finally settles and consolidates (Reed *et al.*, 2008). These processes yield two end-member types of mud: one type that is considered a viscous fluid and another one that is consolidated and can be considered an elasto-plastic material (Foda et al., 1993). Usually, the mud type is defined by the particulates per volume of fluid (g L^{-1}): viscous muds have a density from 10 to 480 g L^{-1} , which corresponds to a density of 1.05 to 1.30 g cm^{-3} . In contrast, consolidated mud exceeds this upper limit (Reed *et al.*, 2008).

According to Reed et al. (2008), in cores 2 and 3, the density ranged between 0.73 and 1.53 g cm^{-3} and 1.10 to 1.29 g cm^{-3} , respectively, while it ranged from 1.33 to 2.03 g cm^{-3} in core 4 (Table S2). The analysis of core 1 was not possible. Therefore, cores 2 and 3 consist of fluid mud, while the density is higher in core 4, suggesting consolidated layers. However, the ^{210}Pb analyses indicate that all cores presented an initial mixed layer of approximately 40 cm. The lack of stable layering prevents any temporal analyses of hydrocarbon contamination in the area, and the reconstruction of a depositional history is not possible. Moreover, storm surges may create gaps in the historical registry through sediment remobilization (Calliari *et al.*, 2000; Calliari et al., 2007; Figueiredo and Calliari, 2006).

Sediments in the Cassino beach mudbank cores were predominantly fine (silt + clay), in agreement with the results reported for the area (Calliari et al., 2007), ranging from 60.0 to 73.5% in core 1, from 18.5 and 87.2% in core 2 and between 65.0 and 93.7% in core 4. Core 3 showed the greatest amount of fine sediments (90.2–100%, Table 1). Total organic carbon varied between 0.09% and 1.56%, with the highest TOC values found in core 3 (Table 1).

3.2.1 - Aliphatic Hydrocarbons

The total AHs levels varied from 11.6 to 35.9 $\mu\text{g g}^{-1}$ (d.w.) in the Cassino Beach mud bank sediment cores (Table 1, Fig. 5). Sediment core 3 showed the highest total AHs concentrations compared to the other cores, ranging from 31.6 $\mu\text{g g}^{-1}$ at the bottom to 35.9 $\mu\text{g g}^{-1}$ at the top. The total AHs concentrations were relatively constant throughout all four sediment cores (Fig. 5), ranging from 32.31 to 31.18 $\mu\text{g g}^{-1}$ in core 1, from 11.62 to 31.23 $\mu\text{g g}^{-1}$ in core 2 and varying from 22.78 to 32.49 $\mu\text{g g}^{-1}$ in core 4.

UCM was present in all analyzed samples and comprised more than 70% of the total Ahs in most samples (Fig. 5). The high abundance of UCM, an indicator of petroleum pollution (Yunker et al., 2002), suggests a chronic petrogenic input in the area. The ratio between UCM and resolved aliphatics can help to identify chronic sources of oil in the sediments ($\text{UCM}/\text{RA} > 4$). This ratio was higher than 4 in 5 samples: at the top of cores 2 and 3 and at the bottom of core 4 (Table 1). The results were below 4 in the majority of samples, indicating the predominance of contributions from higher plants (Bourbonniere et al., 1996). The CPI results were above 1 along all cores and did not suggest petroleum inputs.

The $\Sigma n\text{C}_{12}\text{-}n\text{C}_{36}$ concentrations were relatively low, ranging from < LOQ to 2.77 $\mu\text{g g}^{-1}$. There was no evident trend in *n*-alkane deposition along the cores (Fig. 5). Similar to total AHs, the *n*-alkane concentrations were higher in sediment core 3, with a significant correlation between $\Sigma n\text{C}_{12}\text{-}n\text{C}_{36}$ vs TOC ($r_s = 0.83$;

$p < 0.05$) and $\Sigma nC_{12}-nC_{36}$ vs fine sediments ($r_s = 0.67$; $p < 0.05$) in all cores. Individual n -alkane distributions revealed the predominance of long-chain odd n -alkanes ($C > 23$), indicating input from terrigenous sources. The alk_{ter} ratio results also suggest prominent contributions of higher plants in all cores (Table 1). Similar to the samples collected inside the lagoon, the nC_{31} n -alkane showed the highest concentrations throughout all sediment cores, indicating the predominance of inputs derived from C4-type grasses (Schefuß et al., 2003). Regarding the other proxies for n -alkanes, ACL was similar to the values observed for the estuarine samples, remaining in the range of mixtures of woody and graminoid plants (27.9–30.0). The proxy P_{aq} was also similar to the estuarine area (0.11–0.28), pointing to a mixed source range. Additionally, these proxies presented a homogenous distribution along the cores. The TAR values could not be calculated since short chain n -alkanes (nC_{15} , nC_{17} and nC_{19}) were not detected in any core sediments.

Total AHs and UCM concentrations were relatively constant throughout all four sediment cores, suggesting that either the inputs were constant over time or the sediment layers were mixed due to physical processes, which is more plausible considering the fluid state of the cores, as explained in the section above. This is also corroborated by the lack of short chain n -alkanes and the high percentage of UCM in the cores. The resuspension and mixing of the sediments makes the more labile short chain n -alkanes vulnerable to decomposition, while UCM is more resistant to degradation and is preserved. Therefore, physical processes may influence the record of hydrocarbons stored in mudbank sediments.

3.2.2. Polycyclic Aromatic Hydrocarbons

The Σ_{23} PAH concentrations varied from 7.17 to 33.35 $ng\ g^{-1}$ (d.w.) in core 1, between < LOQ and 18.48 $ng\ g^{-1}$ (d.w.) in core 2 and ranged from 7.11 to 17.47 $ng\ g^{-1}$ (d.w.) in core 4. Similar to AHs, sediment core 3 showed the highest PAH concentrations, with Σ_{23} PAH varying between 69.23 and 119.53 $ng\ g^{-1}$ (d.w.). Overall, the PAHs concentrations along all cores were relatively constant. A significant correlation was observed between total PAHs and TOC ($r_s = 0.78$; $p < 0.05$) and grain size ($r_s = 0.81$, $p < 0.05$) in all cores. The individual PAH distribution showed lower concentrations of LMW PAHs and the dominance of HMW PAHs, with fluoranthene, pyrene and benzo(a)anthracene (4 aromatic rings), benzofluoranthene, benzo(e)pyrene and indeno[1,2,3-c,d]pyrene (5 rings) and benzo[ghi]perylene (6 rings) being the most abundant PAHs (Fig. 6). All the diagnostic ratios indicated combustion as the main source of PAHs in all 4 cores, in particular the combustion of wood, grass or coal (Fig. 4 and Table 1).

Perylene was the most abundant PAH in all layers of all sediment cores, with concentrations varying from < LOQ to 20.35 $ng\ g^{-1}$ (d.w.) in cores 1, 2 and 4 and from 26.67 to 62.91 $ng\ g^{-1}$ (d.w.) in core 3. All samples showed a prevalence of perylene over the $\Sigma 5$ -ring PAHs (more than 69% of perylene), indicating a predominance of diagenetic sources to the Cassino mud bank (Table 1).

3.2.3. – Hydrocarbons distribution

Overall, AHs and PAHs concentrations in the Cassino beach mudbank sediment cores were low, much lower than concentrations found near the main hydrocarbon sources at Patos Lagoon estuary (sites 2–10) and similar to concentrations found in sites located in areas far from the expected sources (sites 1, 11–13) or with low content of fine sediments, such as Manguieira Cove (sites 14–17). The exception was PAHs in core 3, where concentrations were similar to those seen in sites located in the main navigation channel (19–27). The higher contents of fine sediments and TOC may explain the higher levels of PAHs in core 3. However, the lack of LMW PAHs could also suggest that physical processes of mixing sediment, caused by mud fluidity, promote remobilization or degradation of LMW PAHs, which are more susceptible to this process than HMW PAHs. This may explain why there are low concentrations of LMW PAHs and short chain n -alkanes.

3.3 – FINAL CONSIDERATIONS

Hydrocarbons inside the lagoon and in the mudbank seem to have similar sources, showing both biogenic and anthropogenic signatures. Aliphatics indicated the predominance of terrigenous n -alkanes derived from higher plant waxes and chronic inputs of petrogenic sources. Regarding PAHs composition and diagnostic ratios, pyrogenic PAHs were evidenced inside the Patos Lagoon estuary as well as in the adjacent coastal area.

The Patos Lagoon estuary discharge transports high amounts of suspended material to the adjacent coast, being the main source of sediments to the Cassino beach mudbank (Calliari et al., 2009). Thus, considering the similarity between the levels and profiles of individual hydrocarbons in sediments from the estuary and mudbank, it is clear that Patos Lagoon is also the main source of hydrocarbons to the adjacent coastal area. However, all sediment cores showed PAHs concentrations below PEL, TEL Buchman (2008) and threshold limits set by the Brazilian sediment quality guidelines (Brazil, 2012). Therefore, the mud periodically transported by storm surges to Cassino Beach shoreface poses minimal threats to the local biota and beach users regarding PAHs contamination.

4 Conclusions

The hydrocarbon individual distribution, as well as the diagnostic ratios, reveals a mixture of natural and anthropogenic inputs inside the Patos Lagoon estuary and outside the Cassino Beach mudbank. Source proximity seems to be the main cause of the hydrocarbon concentrations observed around the study area, with higher hydrocarbon concentrations observed closer to the main potential sources. According to national (CONAMA 454) and international sediment quality guidelines, 5 sites inside the lagoon were shown to be moderately to highly contaminated. Nevertheless, the mud transported by storm surges to Cassino Beach shoreface showed no threat to local biota and humans, since the sediment cores collected in the mudbank showed hydrocarbons concentrations below the threshold limits of sediment quality guidelines. Although depositional history is not registered in the cores due to physical mixing, it is possible to observe that biogenic n -alkanes derived from terrestrial plants, n -alkanes derived from chronic petrogenic inputs and pyrolytic PAHs contributions are the predominant sources of hydrocarbons to the samples both inside the estuary and in the mud bank. Since the Patos Lagoon estuary is the main source of suspended sediments to the mudbank and the fact that hydrocarbon signatures are similar in both collection areas, it is clear that the

hydrocarbons are being transported to the Cassino beach mudbank through the lagoon discharge channel and that the mud bank is a depositional site for the hydrocarbons originating in the Lagoon.

Declarations

Acknowledgements

The authors acknowledge Dr. Lauro Júlio Calliari for access to the sediment core samples and Dr. José Marcos Godoy at Pontifícia Universidade Católica do Rio de Janeiro for radiochronology and sedimentation rate determinations.

Funding

Patricia Neves (MSc grant 133350/2007-0) and Gilberto Fillmann (PQ 312341/2013-0 and 314202/2018-8) were sponsored by CNPq (Brazilian National Research Council). The authors are also grateful to Petrobras for the financial support (Contract No 650.2.386.03.5).

Authors' contribution

PAN: conceptualization, sample collection, analysis, writing the first draft; PGC: analysis, review, editing; LCP: sample collection, analysis, review, editing; MRG: sample collection, review, editing; GF: conceptualization, review, editing.

Conflict of interest The authors declare no competing interest.

Consent for publication All of the authors consented to publish this manuscript.

Availability of data and materials All data and materials support the published claims and comply with field standards.

References

1. Aboul-Kassim, T.A.T., Simoneit, B. R. T. 1996. Lipid geochemistry of surficial sediments from the coastal environment of Egypt. I. Aliphatic hydrocarbons – characterization and sources. *Marine Chemistry* 54, 135-158.
2. Ankit Y., Mishra P.K., Kumar P., Jha D.K., Kumar V.V., Ambili V., Anoop A. 2017. Molecular distribution and carbon isotope of n-alkanes from Ashtamudi Estuary, South India: Assessment of organic matter sources and paleoclimatic implications. *Marine Chemistry* 196, 62-70.
3. Antônio, Maria; Fernandes, E.; Muelbert, José. 2020. Impact of Jetty Configuration Changes on the Hydrodynamics of the Subtropical Patos Lagoon Estuary, Brazil. *Water*, 12 (11), 3197. DOI: 10.3390/w12113197.
4. Arzayus K.M., Dickhut R.M., Canuel E.A. 2002. Effects of physical mixing on the attenuation of polycyclic aromatic hydrocarbons in estuarine sediments. *Organic Geochemistry* 33, 1759-1769. [https://doi.org/10.1016/S0146-6380\(02\)00120-1](https://doi.org/10.1016/S0146-6380(02)00120-1)
5. Assunção, M. A., Frena, M., Santos, A. P. S., dos Santos Madureira, L. A. 2017. Aliphatic and polycyclic aromatic hydrocarbons in surface sediments collected from mangroves with different levels of urbanization in southern Brazil. *Marine Pollution Bulletin*, 119(1), 439–445. <https://doi.org/10.1016/j.marpolbul.2017.03.071>
6. Baumard, P., Budzinski, H., Garrigues, P. 1998. PAHs in Arcachon Bay, France. origin and biomonitoring with caged organisms. *Mar. Pollut. Bull.* 36, 57–586.
7. Bay S.M., Zeng E.Y., Lorenson T.D., Tran K., Alexander C. 2003. Temporal and spatial distributions of contaminants in sediments of Santa Monica Bay, California. *Marine Environmental Research*. 56, 255-276. [https://doi.org/10.1016/S0141-1136\(02\)00334-3](https://doi.org/10.1016/S0141-1136(02)00334-3)
8. Bayona J.M., Albaigés J. 2006. Sources and Fate of Organic Contaminants in the Marine Environment, 323-370. https://doi.org/10.1007/698_2_010
9. Bi, X.; Sheng, G.; Liu, X.; Li, C.; Fu, J. 2005. Molecular and carbon and hydrogen isotopic composition of n-alkanes in leaf waxes. *Organic Geochemistry* 36, 1405-1417.
10. Bixian M., Jiamo F., Gan Z., Zheng L., Yushun M., Guoying S., Xingmin W. 2001. Polycyclic aromatic hydrocarbons in sediments from the Pearl river and estuary, China: spatial and temporal distribution and sources. *Applied Geochemistry* 16, 1429-1445. [https://doi.org/10.1016/S0883-2927\(01\)00050-6](https://doi.org/10.1016/S0883-2927(01)00050-6)
11. Burchard, H., Schuttelaars, H. M.; Ralston, D. K. 2018. Sediment Trapping in Estuaries. *Annual Review of Marine Science* 10:1, 371-395.
12. Boldrini, I.I., Eggers, L. 1996. Grassland vegetation in Southern Brasil: dynamics of species in cattle excluded areas. *Acta Botanica Brasilica*, v.10, 37-50.
13. Boonyatumanond R., Wattayakorn G., Togo A., Takada H. 2006. Distribution and origins of polycyclic aromatic hydrocarbons (PAHs) in riverine, estuarine, and marine sediments in Thailand. *Marine Pollution Bulletin* 52 942-956 <https://doi.org/10.1016/j.marpolbul.2005.12.015>
14. Bouloubassi I., Saliot A. 1991. Sources and transport of hydrocarbons in the Rhone delta sediments (Northwestern Mediterranean). *Fresenius Journal of Analytic Chemistry* 339, 765-771. <https://doi.org/10.1007/BF00321741>
15. Bourbonniere R.A., Meyers. P.A. 1996. Sedimentary geolipid records of historical changes in the watersheds and productivities of Lakes Ontario and Erie. *Limnology and Oceanography* 4, 352–359.
16. Brasil. 2012. Resolução CONAMA Nº 454, de 01 de novembro de 2012. Estabelece as diretrizes gerais e os procedimentos referenciais para o gerenciamento do material a ser dragado em águas sob jurisdição nacional. Brasília, DF: Conselho Nacional de Meio Ambiente (CONAMA). <http://www.mma.gov.br/port/conama/legiabre.cfm?codlegi=693>. Accessed in March 25th 2018.
17. Buchman, M.F. 2008. NOAA Screening quick reference tables. National Ocean and Atmospheric Administration, Office of Response and Restoration Division (NOAA OR & R Report) 08-1. Seattle, USA. <https://repository.library.noaa.gov/view/noaa/9327>. Accessed in March 25th 2018.

18. Calliari L.J., Holland K.T., Pereira P.S., Guedes R.M.C., Santo R.E. 2007. The influence of mud on the inner shelf, shoreface, beach and surf zone morphodynamics – Casino, southern Brazil. *Coastal Sediments'07*, New Orleans, MS, p. 1-11.
19. Calliari L.J., Speranski N.S., Torronteguy M., Oliveira M.B. 2001. The mud banks of Cassino Beach, Southern Brazil: Characteristics, Processes and Effects. *Journal of Coastal Research*, Coastal Education & Research Foundation, Inc., 2001, pp. 318–25, <http://www.jstor.org/stable/25736298>
20. Calliari L.J., Winterwerp J.C., Fernandes E.H.L., Cuchiara D., Vinzon S.B., Sperle M., Holland K.T. 2009. Fine Grain sediment transport and deposition in the Patos Lagoon-Cassino beach sedimentary system. *Continental Shelf Research*. <https://doi.org/10.1016/j.csr.2008.09.019>.
21. Cardoso, F. D., Dauner, A. L. L., Martins, C. C. 2016. A critical and comparative appraisal of polycyclic aromatic hydrocarbons in sediments and suspended particulate material from a large South American subtropical estuary. *Environmental Pollution*, 214, 219-229. <https://doi.org/10.1016/j.envpol.2016.04.011>.
22. Cavalcante, R. M., Sousa, F. W., Nascimento, R. F., Silveira, E. R., & Freire, G. S. S. 2009. The impact of urbanization on tropical mangroves (Fortaleza, Brazil): evidence from PAH distribution in sediments. *Journal of Environmental Management*, 91(2), 328–335. <https://doi.org/10.1016/j.jenvman.2009.08.020>
23. Chen, C.W., Chen, C.F., 2011. Distribution, origin, and potential toxicological significance of polycyclic aromatic hydrocarbons (PAHs) in sediments of Kaohsiung Harbor, Taiwan. *Marine Pollution Bulletin* 63 (5–12), 417–423. <https://doi.org/10.1016/j.marpolbul.2011.04.047>.
24. Chevalier, N., Savoye, N., Dubois, S., Lama, M. L., David, V., Lecroart, P., Budzinski, H. 2015. Precise indices based on n-alkane distribution for quantifying sources of sedimentary organic matter in coastal systems. *Organic Geochemistry* 88, 69–77. <https://doi.org/10.1016/j.orggeochem.2015.07.006>.
25. Clark JR, R. C.; Blumer, M. 1967. Distribution of n-paraffins in marine organisms and sediment. *Limnol Oceanogr*, v.12, n. 1, 79-87.
26. Culotta L., De Stefano C., Gianguzza A., Mannino M.R., Orecchio S. 2006. The PAH composition of surface sediments from Stagnone coastal lagoon, Marsala (Italy). *Marine Chemistry* 99, 117-127. <https://doi.org/10.1016/j.marchem.2005.05.010>.
27. Dauner, A.L.L., Hernandez, E.A., MacCormack, W.P., Martins, C.C., 2015. Molecular characterisation of anthropogenic sources of sedimentary organic matter from Potter Cove, King George Island, Antarctica. *Science of the Total Environment* 502, 408-416. <https://doi.org/10.1016/j.scitotenv.2014.09.043>.
28. Dyer K.R. 1988. Fine Sediment Particle Transport in Estuaries. In: Dronkers J., van Leussen W. (eds.) *Physical Processes in Estuaries*. Springer, Berlin, Heidelberg.
29. Eglinton G., Hamilton R.J. 1967. Leaf epicuticular waxes. *Science* 156, 1322-1334. <https://doi.org/10.1126/science.156.3780.1322>.
30. Eglinton, G., Gonzalez, A.G., Hamilton, R.J., Raphael, R.A., 1962. Hydrocarbon constituents of the wax coatings of plant leaves: A taxonomic survey. *Phytochemistry* 1, 89–102. [https://doi.org/10.1016/S0031-9422\(00\)88006-1](https://doi.org/10.1016/S0031-9422(00)88006-1).
31. Essien, J.P., Eduok, S.I., Olajire, A.A., 2011. Distribution and ecotoxicological significance of polycyclic aromatic hydrocarbons in sediments from Iko River estuary mangrove ecosystem. *Environmental Monitoring and Assessment* 176 (1–4), 99–107. <https://doi.org/10.1007/s10661-010-1569-2>.
32. Fabbri D., Vassura I., Sun C.G., Snape C.E., McRae C., Fallick A.E. 2003. Source apportionment of polycyclic aromatic hydrocarbons in a coastal lagoon by molecular and isotopic characterisation. *Marine Chemistry* 84, 123-135. [https://doi.org/10.1016/S0304-4203\(03\)00135-X](https://doi.org/10.1016/S0304-4203(03)00135-X)
33. Fahl, K.; Stein, R. 1997. Modern organic carbon deposition in Laptev Sea and adjacent continental slope: surface water productivity vs. terrigenous input. *Organic Geochemistry*, 26, 379-390.
34. Farias, C. O., Hamacher, C., Wagener, A. de L. R., & Scofield, A. de L. 2008. Origin and degradation of hydrocarbons in mangrove sediments (Rio de Janeiro, Brazil) contaminated by an oil spill. *Organic Geochemistry*, 39, 289–307. <https://doi.org/10.1016/j.orggeochem.2007.12.008>
35. Figueiredo S.A., Calliari L.J. 2006. Sedimentologia e suas implicações na morfodinâmica das praias adjacentes às desembocaduras na linha de costa do Rio Grande do Sul. *Gravel* 4, 73-87. http://www.ufrgs.br/gravel/4/Gravel_4_06.pdf. Accessed in March 25th 2018.
36. Foda M., Hunt J.R., Chou H.T. 1993. A nonlinear model for the fluidization of marine mud by waves. *Journal of Geophysical Research-Oceans* 98, 7039-7047. <https://doi.org/10.1029/92JC02797>.
37. Gale S.J., Haworth R.J., Pisanu P.C. 1995. The 210Pb chronology of late holocene deposition in an Eastern Australian Lake basin. *Quaternary Science Reviews* 14, 395-408. [https://doi.org/10.1016/0277-3791\(95\)00033-X](https://doi.org/10.1016/0277-3791(95)00033-X).
38. Garcia, M.R., Mirlean, N., Baisch, P.R., Caramão, E.B. 2010. Assessment of polycyclic aromatic hydrocarbon influx and sediment contamination in an urbanized estuary. *Environ Monit Assess* 168, 269–276. <https://doi.org/10.1007/s10661-009-1110-7>
39. Garcia, C.A.E., Evangelista, H., Möller, O.O. Jr. 2021. "Comments on "Dredging in an estuary causes contamination by fluid mud on a tourist ocean beach. Evidence via REE ratios" by N. Mirlean, L. Calliari, and K. Johannesson in *Marine Pollution Bulletin* 159 (2020) 111495. <https://doi.org/10.1016/j.marpolbul.2020.111495>." doi: 10.1016/j.marpolbul.2021.112115.
40. Goswami, P., Ohura, T., Guruge, K.S., Yoshioka, M., Yamanaka, N., Akiba, M., Munuswamy, N. 2016. Spatio-temporal distribution, source, and genotoxic potential of polycyclic aromatic hydrocarbons in estuarine and riverine sediments from southern India. *Ecotoxicol. Environ. Saf.* 130, 113–123. <https://doi.org/10.1016/j.ecoenv.2016.04.016>
41. Gray, J.S. 1981. *The Ecology of Marine Sediments - An Introduction to the Structures and Functions of Benthic Communities*. Cambridge, University Press, New York. ISBN 0-521-28027-3. 185 pp
42. Holland, K. T., Vinzon, S. B., Calliari, L. J. 2009. A field study of coastal dynamics on a muddy coast offshore of Cassino beach, Brazil. *Continental Shelf Research* 29, 503–514. <https://doi.org/10.1016/j.csr.2008.09.023>
43. Hostettler F.D., Pereira W.E., Kvenvolden K.A., van Geen A., Luoma S.N., Fuller C.C., Anima R. 1999. A record of hydrocarbon input to San Francisco Bay as traced by biomarker profiles in surface sediment and sediment cores. *Marine Chemistry* 64, 115-127. [https://doi.org/10.1016/S0304-4203\(98\)00088-7](https://doi.org/10.1016/S0304-4203(98)00088-7).
44. Janeiro, J.; Fernandes, E.; Martins, F.; Fernandes, R. 2008. Wind and freshwater influence over hydrocarbon dispersal on Patos Lagoon, Brazil. *Marine Pollution Bulletin* 56 (4), 650-665. <https://doi.org/10.1016/j.marpolbul.2008.01.011>.

45. Jeng W.-L. 2006. Higher plant *n*-alkane average chain length as an indicator of petrogenic hydrocarbon contamination in marine sediments, *Marine Chemistry* 102, 242–251.
46. Kennish M.J. 1997. *Practical handbook of estuarine and marine pollution*. CRC Press, 524 p. ISBN: 9780849384240
47. Kim, A.W., Vane, C.H., Moss-Hayes, V., Engelhart, S.E., Kemp, A.C. 2017. PAH, PCB, TPH and mercury in surface sediments of the Delaware River Estuary and Delmarva Peninsula, USA. *Marine Pollution Bulletin* 129 (2), 835–845. <https://doi.org/10.1016/j.marpolbul.2017.10.008>
48. Kjerfve, B. 1986. Comparative oceanography of coastal lagoons, p. 63-81. In: Wolfe, D.A. ed. *Estuarine Variability*. New York, Academic Press. 509p.
49. Kumar, K.S.S., Nair, S.M., Salas, P.M., Peter, K.J.P., Kumar, C.S.R. 2016. Aliphatic and polycyclic aromatic hydrocarbon contamination in surface sediment of the Chitrapuzha River, South West India. *Chemistry and Ecology* 32 (2), 117–135. <https://doi.org/10.1080/02757540.2015.1125890>
50. Langston, W., Ridgway, J. 2006. Geological and Geochemistry Influence on the estuarine ecosystems. Chapter 4, pp. 21-48. In: Zektser I.S., Marker B., Ridgway J., Rogachevskaya L., Vartanyan G. (eds) *Geology and Ecosystems*. Springer, Boston, MA. https://doi.org/10.1007/0-387-29293-4_4
51. Lippiatou E., Tolosa I., Simo R., Bouloubassi I., Dachs J., Marti S., Sicre M.-A., Bayona J.M., Grimalt J.O., Salot A., Albaiges J. 1997. Mass budget and dynamics of polycyclic aromatic hydrocarbons in the Mediterranean Sea. *Deep Sea Research Part II: Topical Studies in Oceanography* 44, 881-905. [https://doi.org/10.1016/S0967-0645\(96\)00093-8](https://doi.org/10.1016/S0967-0645(96)00093-8)
52. Marangoni, J.C., Costa, C.S.B. 2009. Natural and anthropogenic effects on salt marsh over five decades in the Patos Lagoon (Southern Brazil). *Brazilian Journal of Oceanography*, 57, 345-350.
53. Marini, M., Frapiccini, E. 2014. Do lagoon area sediments act as traps for polycyclic aromatic hydrocarbons? *Chemosphere*, 111, 80–88. <https://doi.org/10.1016/j.chemosphere.2014.03.037>
54. Martelo, A.F.; Trombetta, T.B.; Lopes, B.V.; Marques, W.C.; Möller, O.O. 2019. Impacts of dredging on the hydromorphodynamics of the Patos Lagoon estuary, southern Brazil. *Ocean Engineering* 188, 106325. <https://doi.org/10.1016/j.oceaneng.2019.106325>.
55. Martins, C. C., Doumer, M. E., Gallice, W. C., Dauner, A. L. L., Cabral, A. C., Cardoso, F. D., Dolci, N. N., Camargo, L. M., Ferreira, P. A. L., Figueira, R. C. L., Mangrich, A. S. 2015. Coupling spectroscopic and chromatographic techniques for evaluation of the depositional history of hydrocarbons in a subtropical estuary. *Environmental Pollution*, 205, 403–414. <https://doi.org/10.1016/j.envpol.2015.07.016>
56. Martins, C.C., Bicego, M.C., Figueira, R.C.L., Angelli, J.L.F., Combi, T., Gallice, W.C., Mansur, A. V., Nardes, E., Rocha, M.L., Wisniewski, E., Ceschim, L.M.M., Ribeiro, A.P. 2012. Multi-molecular markers and metals as tracers of organic matter inputs and contamination status from an Environmental Protection Area in the SW Atlantic (Laranjeiras Bay, Brazil). *Science of the Total Environment* 417–418, 158–168. <https://doi.org/10.1016/j.scitotenv.2011.11.086>
57. Martins, C.C., Seyffert, B.H., Braun, J.F., Fillmann, G. 2011. Input of organic matter in a large South American tropical estuary (Paranaguá Estuarine System, Brazil) indicated by sedimentary sterols and multivariate statistical approach. *Journal of the Brazilian Chemical Society* 22, 1585–1594. <https://doi.org/10.1590/S0103-50532011000800023>
58. Martins, C.C.; Bicego, M.C.; Rose, N.L.; Taniguchi, S.; Lourenço, R.A., Figueira, R.C.L., Mahiques, M.M., Montone, R.C. 2010. Historical record of polycyclic aromatic hydrocarbons (PAHs) and spheroidal carbonaceous particles (SCPs) in marine sediment cores from Admiralty Bay, King George Island, Antarctica. *Environmental Pollution*, 158, 158-200. <https://doi.org/10.1016/j.envpol.2009.07.025>
59. Massone, C.G., Wagener, A. de L.R., de Abreu, H.M., and Veiga, Á. 2013. Revisiting hydrocarbons source appraisal in sediments exposed to multiple inputs. *Marine Pollution Bulletin* 73(1), 345–354. <https://doi.org/10.1016/j.marpolbul.2013.05.043>
60. Matthiensen A., Yunes J.S., Codd G.A. 1999. Ocorrência, distribuição e toxicidade de cianobactérias no estuário da Lagoa dos Patos, RS. *Revista Brasileira de Biologia* 59, 361-376. <https://doi.org/10.1590/S0034-71081999000300002>
61. Medeiros P.M., Bicego M.C., Castela R.M., Rosso C.D., Fillmann G., Zamboni A.J. 2005. Natural and anthropogenic hydrocarbons inputs to sediments of Patos Lagoon Estuary, Brazil. *Environment International* 31, 77-87. <https://doi.org/10.1016/j.envint.2004.07.001>
62. Medeiros, P.M., Bicego, M.C., 2004. Investigation of natural and anthropogenic hydrocarbon inputs in sediments using geochemical markers. I. Santos, SP – Brazil. *Marine Pollution Bulletin* 49, 761–769. <https://doi.org/10.1016/j.marpolbul.2004.06.001>
63. Meyers, P. A. 1997. Organic geochemical proxies of paleoceanographic, paleolimnologic, and paleoclimatic processes. *Organic Geochemistry* 27, 213-250. [https://doi.org/10.1016/S0146-6380\(97\)00049-1](https://doi.org/10.1016/S0146-6380(97)00049-1)
64. Mirlean, N.; Calliari, L.; Johannesson, N. 2020. Dredging in an estuary causes contamination by fluid mud on a tourist ocean beach. Evidence via REE ratios. *Marine Pollution Bulletin*, 159, 111495. <https://doi.org/10.1016/j.marpolbul.2020.111495>
65. Mitra S., Dellapenna T.M., Dickhut R.M. 1999. Polycyclic Aromatic Hydrocarbon Distribution within Lower Hudson River Estuarine Sediments: Physical Mixing vs Sediment Geochemistry. *Estuarine, Coastal and Shelf Science* 49, 311-326. <https://doi.org/doi.org/10.1006/ecss.1999.0502>
66. Mônica Wallner-Kersanach, M., Mirlean, N., Baumgarten, M.G.Z., Costa, L.D.F., Baisch, P. 2016. Temporal evolution of the contamination in the southern area of the Patos Lagoon estuary, RS, Brazil. *Integrated Coastal Zone Management* volume 16, issue 3, 263-279.
67. Neff J.M. 1979. *Polycyclic aromatic hydrocarbons in the aquatic environment: Sources, fates, and biological effects*. Applied Science Publishers, London, UK, 262 pp. ISBN: 0853348324
68. Niencheski L.F.H., Fillmann G. 2006. Contaminantes: Metais, Hidrocarbonetos e Organoclorados. In: Lana PC, Bianchini A, Ribeiro CAO, Niencheski LFH, Fillmann G, Santos CSG, Editors. *Avaliação Ambiental de estuários brasileiros: diretrizes metodológicas*. Museu Nacional, Rio de Janeiro, 63-118. ISBN: 8574270172
69. Notar M., Leskovsek H., Faganeli J. 2001. Composition, distribution and sources of polycyclic aromatic hydrocarbons in sediments of the Gulf Of Trieste, Northern Adriatic Sea. *Marine Pollution Bulletin* 42, 36-44. [https://doi.org/doi.org/10.1016/S0025-326X\(00\)00092-8](https://doi.org/doi.org/10.1016/S0025-326X(00)00092-8)
70. Oyo-Ita, O. E., Offem, J. O., Ekpo, B. O., & Adie, P. A. 2013. Anthropogenic PAHs in mangrove sediments of the Calabar River, SE Niger Delta, Nigeria. *Applied Geochemistry*, 28, 212–219. <https://doi.org/10.1016/J.APGEOCHEM.2012.09.011>

71. Paixao, J. F., de Oliveira, O. M., Dominguez, J. M., Coelho, A. C., Garcia, K. S., Carvalho, G. C., Magalhaes, W. F. 2010. Relationship of metal content and bioavailability with benthic macrofauna in Camamu Bay (Bahia, Brazil). *Marine Pollution Bulletin*, 60, 474–481. <https://doi.org/10.1016/j.marpolbul.2009.12.002>
72. Ramzi, A., Habeeb Rahman, K., Gireeshkumar, T.R., Balachandran, K.K., Jacob, C., Chandramohanakumar, N., 2017. Dynamics of polycyclic aromatic hydrocarbons (PAHs) in surface sediments of Cochin estuary, India. *Mar. Pollut. Bull.* 114, 1081–1087. <https://doi.org/10.1016/j.marpolbul.2016.10.015>
73. Ravindra, K., Sokhi, R., Van Grieken, R., 2008. Atmospheric polycyclic aromatic hydrocarbons: Source attribution, emission factors and regulation. *Atmos. Environ.* 42, 2895–2921. <https://doi.org/10.1016/j.atmosenv.2007.12.010>
74. Readman J.W., Mantoura R.F.C., Rhead M.M., Brown L. 1982. Aquatic distribution and heterotrophic degradation of polycyclic aromatic hydrocarbons (PAH) in the Tamar estuary. *Estuarine, Coastal and Shelf Science* 14, 369-389. [https://doi.org/10.1016/S0272-7714\(82\)80009-7](https://doi.org/10.1016/S0272-7714(82)80009-7)
75. Readman, J.W., Fillmann, G., Tolosa, I., Bartocci, J., Villeneuve, J.P., Catinni, C., Mee, L.D., 2002. Petroleum and PAH contamination of the Black Sea. *Mar. Pollut. Bull.* 44, 48–62. [https://doi.org/10.1016/S0025-326X\(01\)00189-8](https://doi.org/10.1016/S0025-326X(01)00189-8)
76. Reed A.H., Faas R.W., Allison M.A., Calliari L.J., Holland K.T., O'Reilly S.E., Vaughan W.C., Alvez A. 2009. Characterization of a Mud Deposit Offshore of the Patos Lagoon, Southern Brazil. *Continental Shelf Research* 29, 597 - 608. <https://doi.org/10.1016/j.csr.2009.02.001>
77. Resmi, P., Manju, M. N., Gireeshkumar, T. R., Ratheesh Kumar, C. S., Chandramohanakumar, N. 2016. Source characterisation of Sedimentary organic matter in mangrove ecosystems of northern Kerala, India: Inferences from bulk characterisation and hydrocarbon biomarkers. *Regional Studies in Marine Science*, 7, 43–54. <https://doi.org/10.1016/J.RSMA.2016.05.006>
78. Ridgway J., Shimmield G. 2002. Estuaries as Repositories of Historical Contamination and their Impact on Shelf Seas. *Estuarine, Coastal and Shelf Science* 55, 903-928. <https://doi.org/10.1006/ecss.2002.1035>
79. Schefuß, E., Schouten, S., Jansen, J.H.F. Damsté, J.S. 2003. African vegetation controlled by tropical sea surface temperatures in the mid-Pleistocene period. *Nature*, v.422, n.6930, 418-421.
80. Seeliger U. 2001. The Patos Lagoon Estuary, Brazil. In: Seeliger U., Kjerfve B. (eds) *Coastal Marine Ecosystems of Latin America. Ecological Studies (Analysis and Synthesis)*, vol 144. Springer, Berlin, Heidelberg
81. Sericano, J.L., Brook, J.M., Champ, M.A., Kennicutt, M.C., Makey, V.V., 2001. Trace contaminant concentrations in the Kara Sea and its adjacent rivers, Russia. *Marine Pollution Bulletin* 42, 1017–1030. [https://doi.org/10.1016/S0025-326X\(00\)00236-8](https://doi.org/10.1016/S0025-326X(00)00236-8)
82. Silliman J.E., Meyers P.A., Bourbonniere R.A. 1996. Record of postglacial organic matter delivery and burial in sediments of Lake Ontario. *Organic Geochemistry* 24, 463-472.
83. Silliman J.E., Meyers P.A., Eadie B.J. 1998. Perylene: an indicator of alteration processes or precursor materials? *Organic Geochemistry* 29, 1737-1744. [https://doi.org/10.1016/S0146-6380\(98\)00056-4](https://doi.org/10.1016/S0146-6380(98)00056-4)
84. Tissot, B.P., Welte, D.H. 1978. Geochemical fossils and their significance in petroleum formation. *Petroleum formation and occurrence*. New York, Springer-Verlag; 92–122. <https://doi.org/10.1007/978-3-642-87813-8>
85. Vaezzadeh V., Zakaria M.P., Shau-Hwai A.T., Ibrahim Z.Z., Mustafa S., Abootalebi-Jahromi F., Masood N., Magam S.M., Alkhadher, S.A.A. 2015. Forensic investigation of aliphatic hydrocarbons in the sediments from selected mangrove ecosystems in the west coast of Peninsular Malaysia. *Marine Pollution Bulletin* 100, 311-320. <https://doi.org/10.1016/j.marpolbul.2015.08.034>
86. Varnosfaderany, M.N., Bakhtiari, A.R., Gu, Z., Chu, G., 2014. Perylene as an indicator of land-based plant biomarkers in the southwest Caspian Sea. *Mar. Pollut. Bull.* 80: 124–131. <https://doi.org/10.1016/j.marpolbul.2014.01.033>.
87. Venkatesan M.I. 1988. Occurrence and possible sources of perylene in marine sediments - a review. *Marine Chemistry* 25, 1-27. [https://doi.org/10.1016/0304-4203\(88\)90011-4](https://doi.org/10.1016/0304-4203(88)90011-4)
88. Vinzon, S.B., Lauro, J.C., Holland, K.T., Winterwerp, J.C., 2009. On the dynamics of mud deposits in coastal areas. *Continental Shelf Research* 29 (3), 501–502. <https://doi.org/10.1016/j.csr.2008.09.021>
89. Volkman J.K., Holdsworth G.D., Neil G.P., Bavor H.J.Jr. 1992. Identification of natural, anthropogenic and petroleum hydrocarbons in aquatic sediments. *Science of the Total Environment* 112, 203-219. [https://doi.org/10.1016/0048-9697\(92\)90188-X](https://doi.org/10.1016/0048-9697(92)90188-X)
90. Wallner-Kersanach, M., Mirlean, N.; Baumgarten, M.G.Z.; Costa, L.D.F.; Baisch, P., 2016. Temporal evolution of the contamination in the southern area of the Patos Lagoon estuary, RS, Brazil. *Journal of Integrated Coastal Zone Management*, 16:263-279. <https://doi.org/10.5894/rgci596>
91. Wang X.C., Zang Y.X., Chen R.F. 2001. Distribution and partitioning of polycyclic aromatic hydrocarbons (PAHs) in different size fractions in sediments from Boston Harbor, United States. *Marine Pollution Bulletin* 42, 1139-1149. [https://doi.org/10.1016/S0025-326X\(01\)00129-1](https://doi.org/10.1016/S0025-326X(01)00129-1)
92. Wang, Z., Fingas, M., Page, D.S., 1999. Oil spill identification. *Journal of Chromatography A* 843, 369–411. [https://doi.org/10.1016/S0021-9673\(99\)00120-X](https://doi.org/10.1016/S0021-9673(99)00120-X)
93. White, K.H.; Xu, L.; Hartmann, P.; Quinn, J.G.; Reddy, C.M., 2013. Unresolved Complex Mixture (UCM) in Coastal Environments is derived from Fossil Sources. *Environmental Science and Technology*, 47, 2, 726-731. <https://doi.org/10.1021/es3042065>
94. Wu Y., Zhang J., Mi T.Z., Li B. 2001. Occurrence of n-alkanes and polycyclic aromatic hydrocarbons in the core sediments of the Yellow Sea. *Marine Chemistry* 76, 1-15. [https://doi.org/10.1016/S0304-4203\(01\)00040-8](https://doi.org/10.1016/S0304-4203(01)00040-8)
95. Yang J.-P., Liu X.-P., Zhang J.-W. 1998. Distribution of dibenzothiophene in the sediments of the South China Sea. *Environmental Pollution* 101, 405-414. [https://doi.org/10.1016/S0269-7491\(98\)00020-7](https://doi.org/10.1016/S0269-7491(98)00020-7)
96. Yunes J.S., Salomon P.S., Matthiensen A., Beattie K.A., Raggett S.L., Codd G.A. 1996. Toxic blooms of cyanobacteria in the Patos Lagoon Estuary, southern Brazil. *Journal of Aquatic Ecosystem Stress and Recovery* 4, 223-229. <https://doi.org/10.1007/BF00662183>

97. Yunker, M.B., Macdonald R.W., Vingarzan R., Mitchell R.H., Goyette D., Sylvestre S. 2002. PAHs in the Fraser River basin: a critical appraisal of PAH ratios as indicators of PAH source and composition. *Organic Geochemistry* 33, 489-515. [https://doi.org/10.1016/S0146-6380\(02\)00002-5](https://doi.org/10.1016/S0146-6380(02)00002-5)
98. Zhang, J.D., Wang, Y.S., Cheng, H., Jiang, Z.Y., Sun, C.C., Wu, M.L., 2015. Distribution and sources of the polycyclic aromatic hydrocarbons in the sediments of the Pearl River estuary, China. *Ecotoxicology* 24 (7–8), 1643–1649. DOI: 10.1007/s10646-015-1503-z

Figures

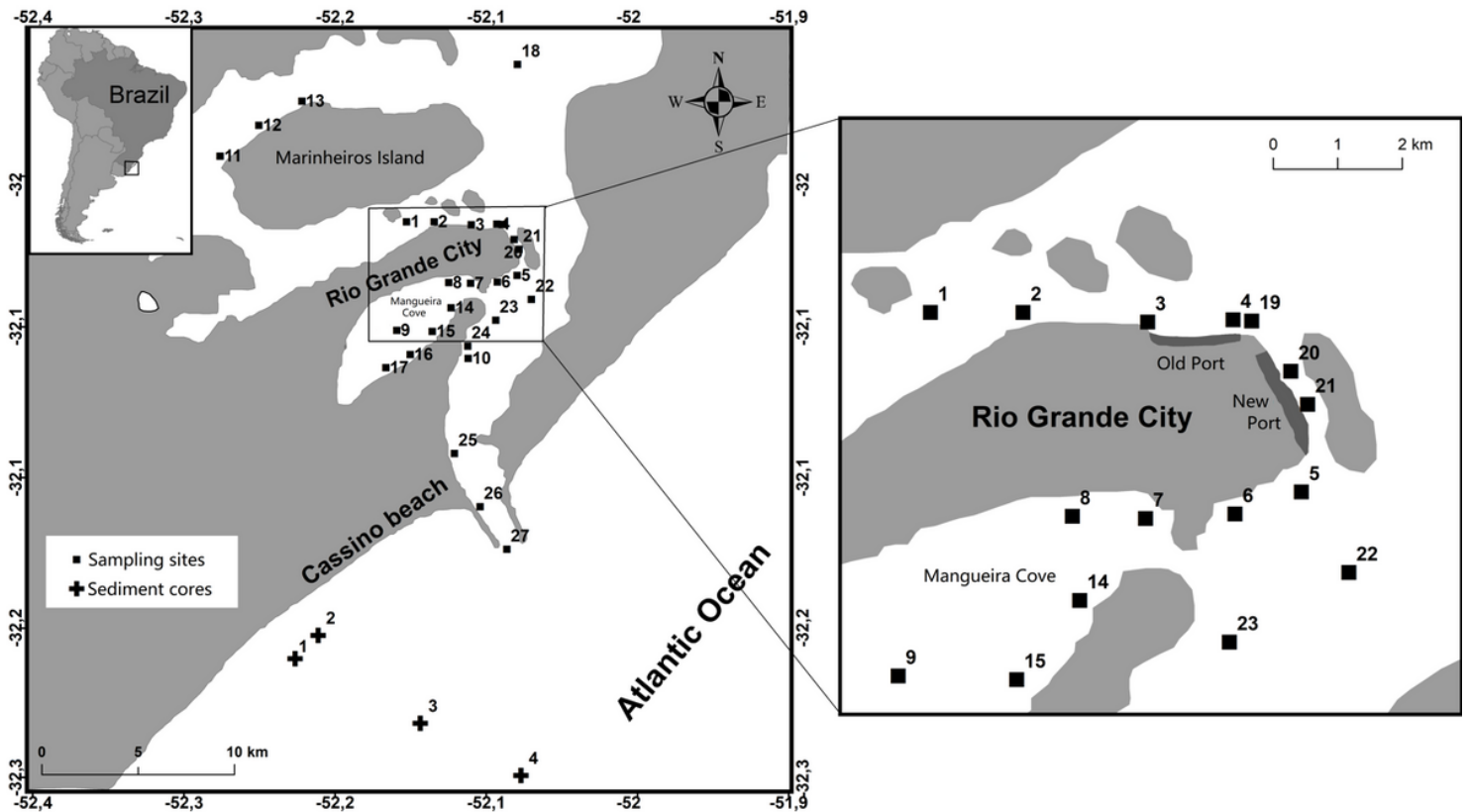


Figure 1

Study area and sampling sites: ■ - surface samples inside the Patos Lagoon estuary and + - sediment cores at the Cassino Beach mudbank.

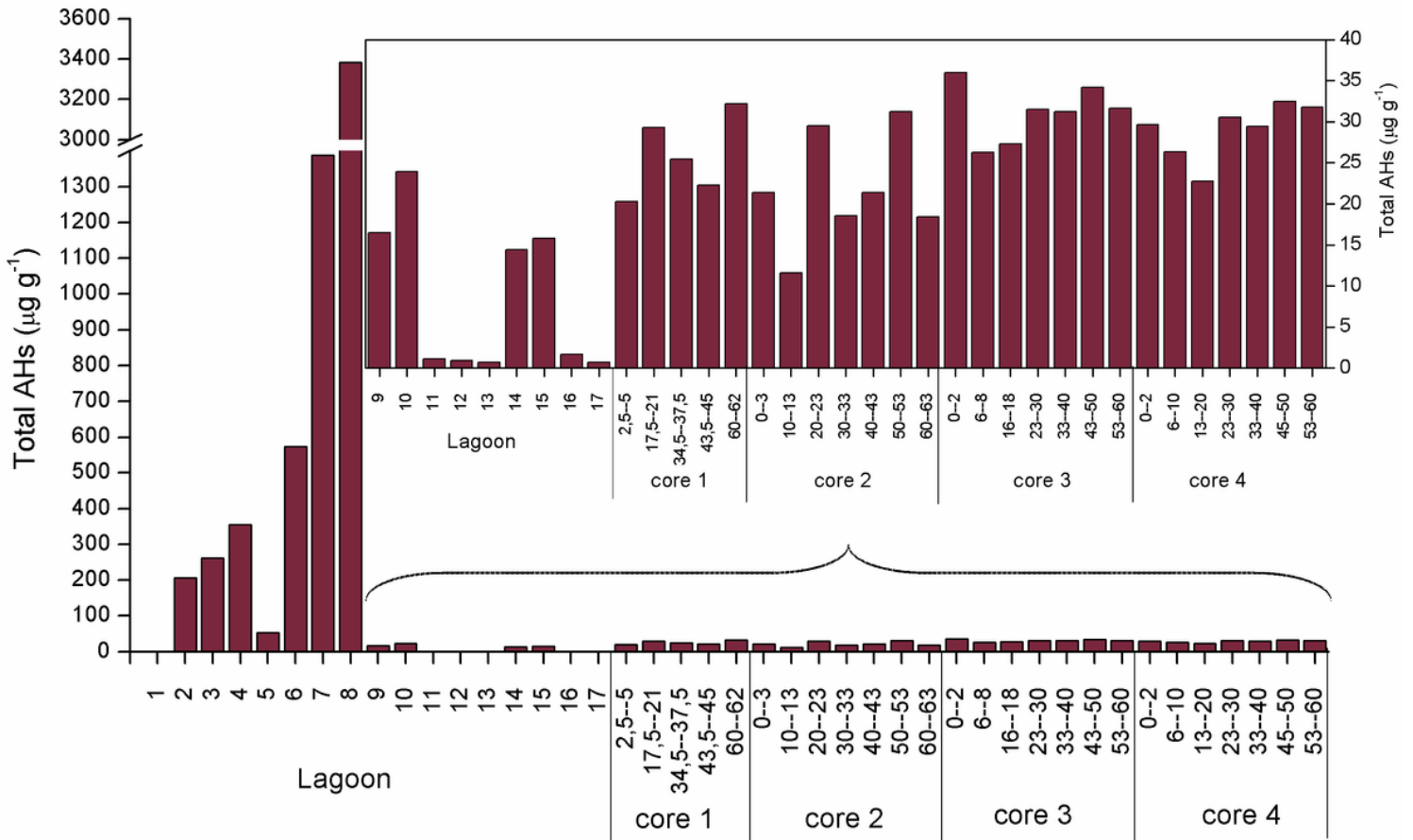


Figure 2
 Total aliphatic concentration ($\mu\text{g g}^{-1}$) in surface sediments sampled inside Patos Lagoon and in the sediment cores collected in Cassino beach mudbank. Aliphatics were not analyzed at sites 18 to 27.

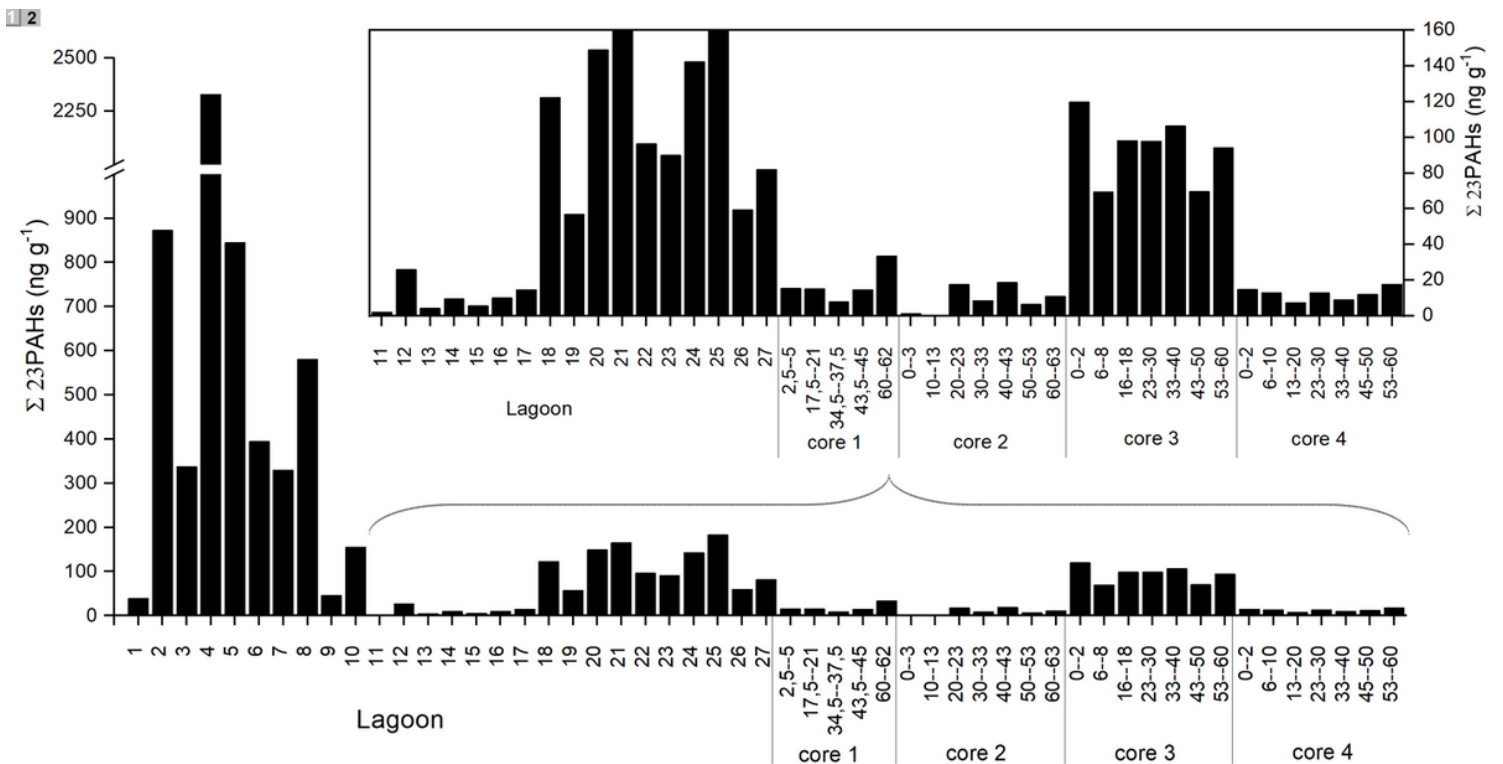


Figure 3

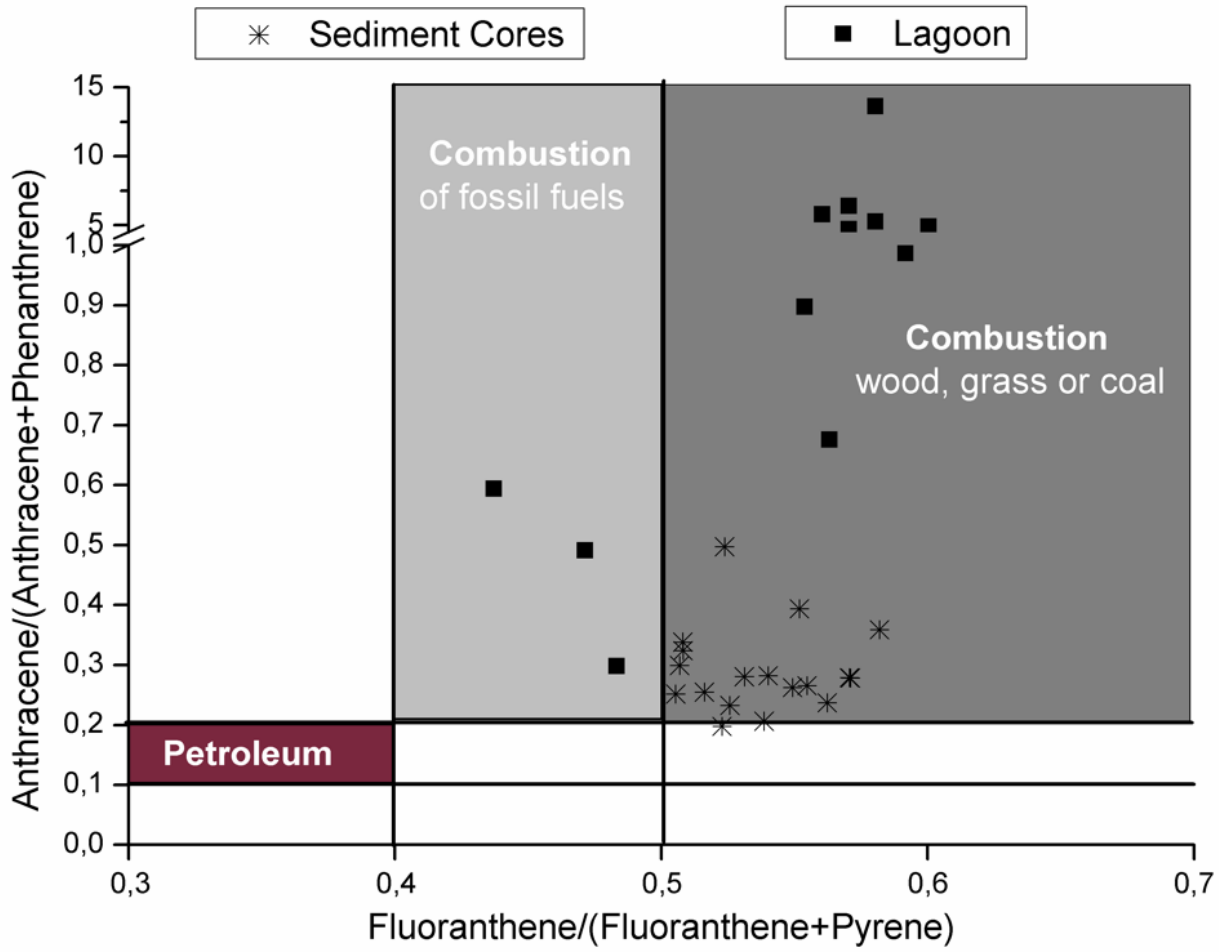


Figure 4
Crossplot of fluoranthene/(fluoranthene+pyrene) and anthracene/(anthracene+phenanthrene) ratios for surface sediments of Patos Lagoon estuary (■) and Cassino beach mudbank sediment cores (*).

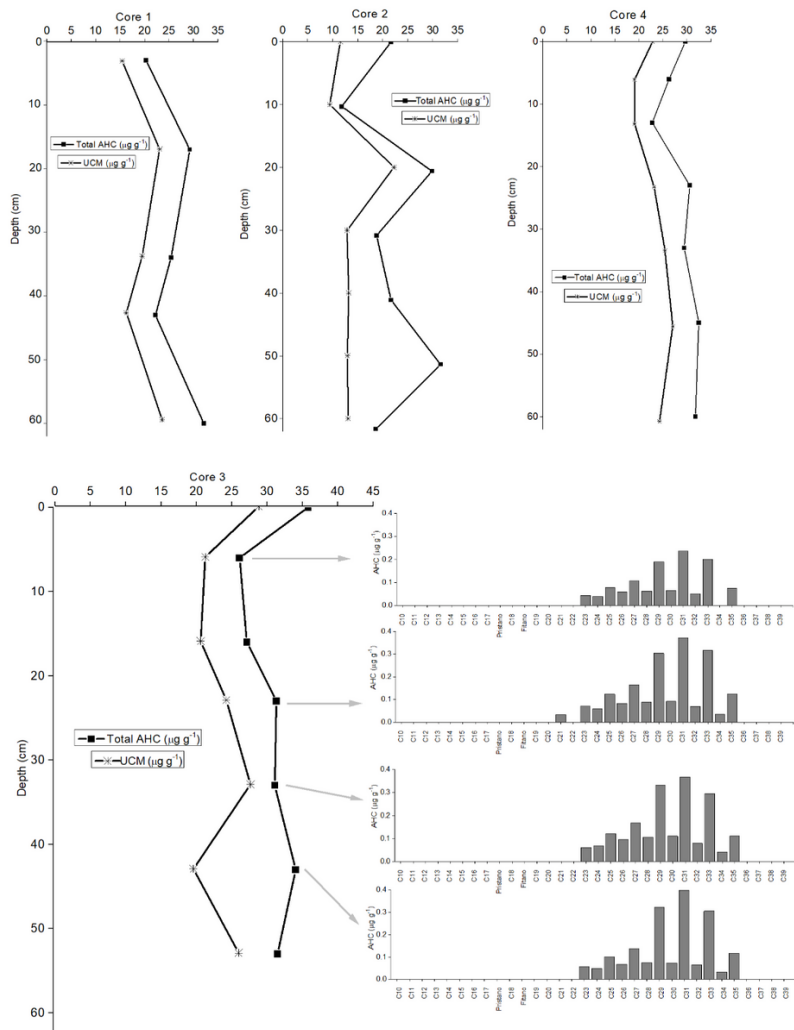


Figure 5

Sedimentary profile of total AHC and UCM (µg g⁻¹) in the Cassino Beach mud bank sediment cores. The individual distribution of alkanes is presented for the selected profile depth of core 3.

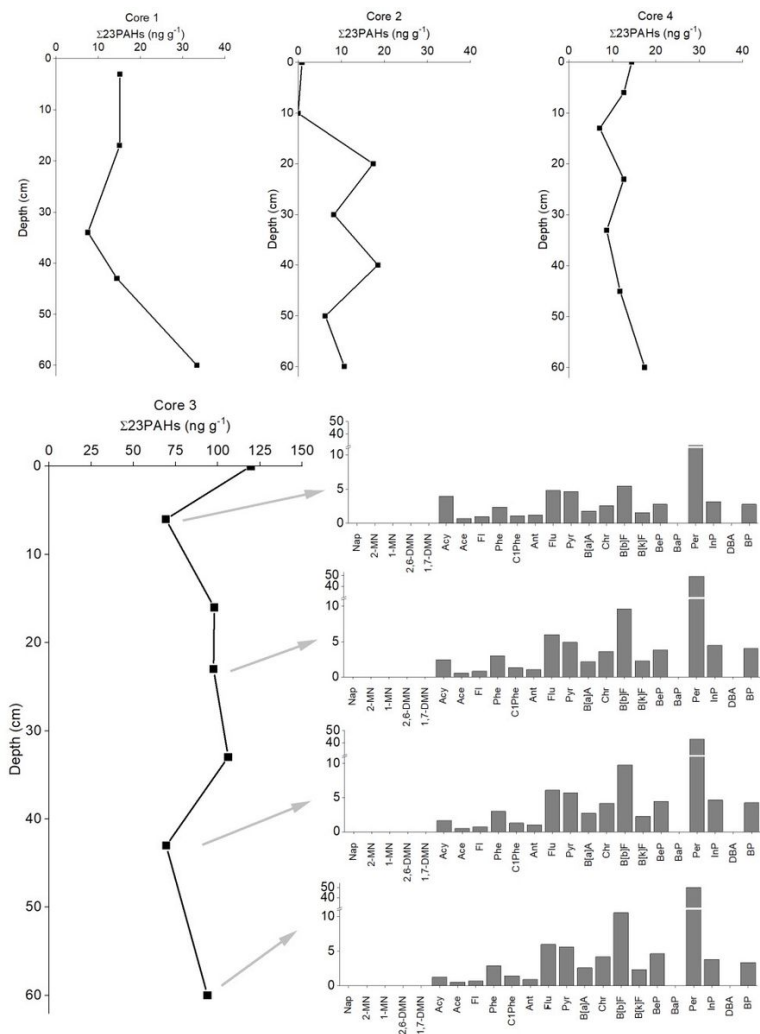


Figure 6
 Sedimentary profile of Σ_{23} PAHs (ng g^{-1}) in the Cassino Beach mud bank sediment cores. The individual distribution of PAHs is presented for the selected profile depth of core 3.

Supplementary Files

This is a list of supplementary files associated with this preprint. Click to download.

- [SUPPORTINFORMATION4.docx](#)